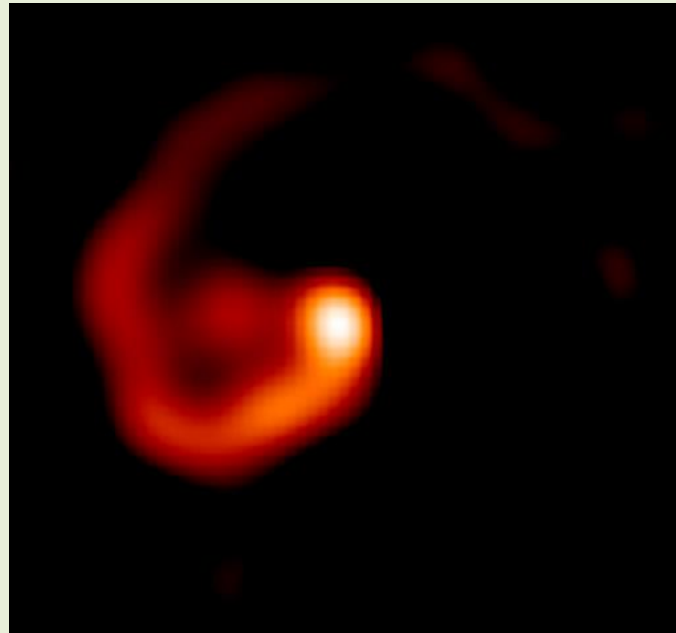


# Variability of Si IV and C IV broad absorption and emission lines of Hot Emission stars, Wolf-Rayet stars, Cataclysmic Variables and Quasars using GR model and ASTA software

**Dr E. Lyratzi**

D. Stathopoulos, E. Danezis, A. Antoniou and D. Tzimeas  
National and Kapodistrian University of Athens, Faculty of Physics,

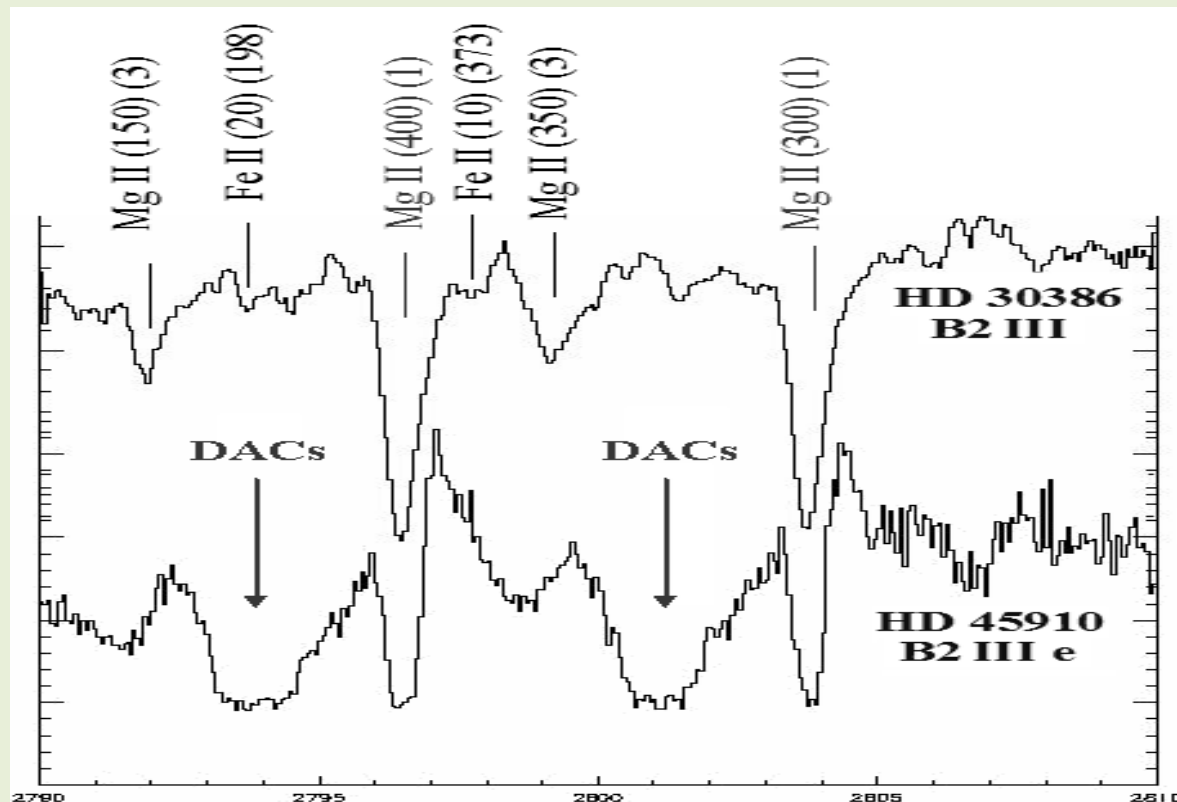


# Discrete Absorption Components (DACs)

In the spectra of **Hot Emission Stars (O and B stars,  $T_{\text{eff}} \geq 10,000$  K)** we observe independent absorption components blueshifted from the corresponding emission lines. We call these absorption spectral lines, **Discrete Absorption Components (DACs)** (Underhill 1975; Henrichs 1984; Underhill & Fahey 1984; Bates & Halliwell 1986; Grady et al. 1987; Lamers et al. 1988; Waldron et al. 1992, 1994; Cranmer & Owocki 1996; Rivinius et al. 1997; Kaper et al. 1996, 1997, 1999; Markova 2000; Cranmer et al. 2000; Danezis et al. 2003, 2007, 2009; Lyratzi et al. 2007).

DACs are spectral lines of the same ion, with **different velocity shifts**, as they are created in different density regions (Danezis 1983, 1987, Danezis et al. 1991, 2003, 2007; Lyratzi & Danezis 2004; Lyratzi et al. 2007).

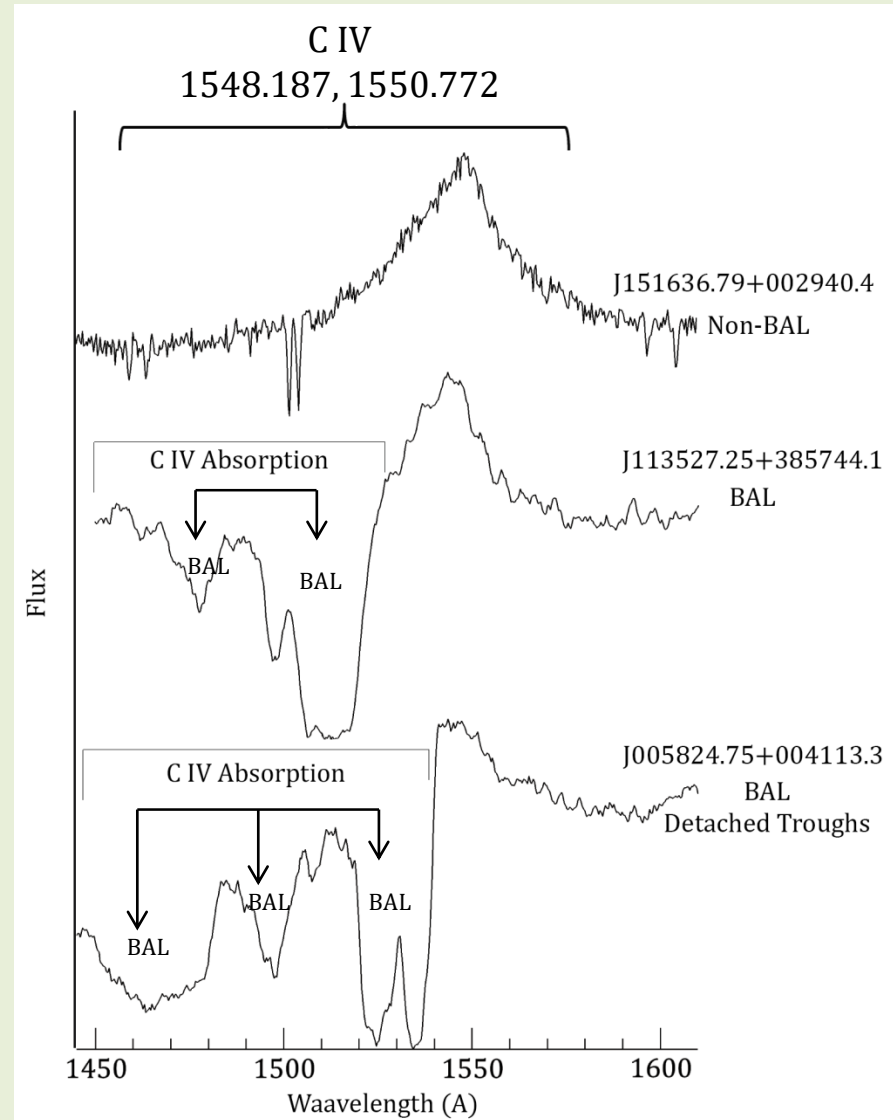
These lines have **very complex** profiles that can not be theoretically reproduced with a known distribution, such as Gaussian, Voigt, or Lorentzian.



# Broad Absorption Lines (BALs)

About 20%-30% of the detected **quasar** population exhibits **Broad Absorption Line (BAL)** troughs blueshifted with respect to the corresponding emission lines in their rest frame UV spectra (Foltz et al. 1990; Hewett & Foltz 2003; Reichard et al. 2003).

BALs are usually observed in high ionization species such as N V, Ly, C IV, Si IV and are sometimes detected in lower ionization species like Mg II or Al III.



# The origin of DACs and BALs.

There are two opposing opinions about the origin of DACs and BALs:

- i. a **smooth continuous flow** with the intensity depending only on optical depth effects (complete source coverage)

(Henrichs 1984; Prinja & Howarth 1986; Prinja et al. 1987; Henrichs et al. 1988; Murray & Chiang 1995) .

- i. a **flow of many individual clouds** which are optically thick and very small compared with the size of the central continuum source.

(Lucy & Solomon 1970; McKee, & Tarter 1975; MacGregor et al. 1979; Carlberg 1980; Lucy 1984; Lucy & White 1980; Owocki & Rybicki 1984, 1985, 1986; Turnshek 1984; Danezis et al. 2003, 2007, 2009; Lyratzi et al. 2009, 2010, 2011; Hamann et al. 2013; Capellupo, Hamann & Barlow 2014),

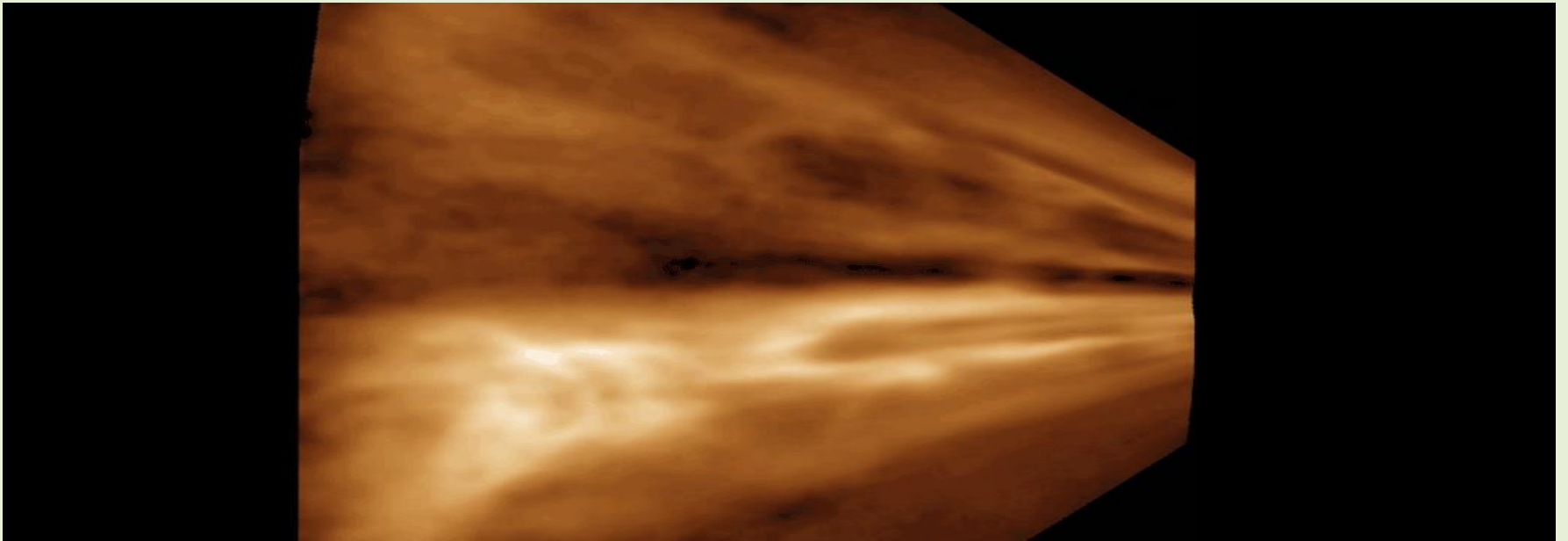
# The origin of DACs

## The case of Hot Emission Stars

**Winds** have been observed in UV spectra, through the P-Cygni profile (Henrichs 1984; Prinja & Howarth 1986; Prinja et al. 1987; Henrichs et al. 1988).

However, **the models of normal winds can not interpret the structure of the regions where DACs are created.**

Besides, we know that the e phenomenon (i.e. the emission lines) is due to the **violent mass ejection** in the equatorial plane when the rotational velocity of the star reaches a critical value which disrupt the smooth outflow.



# The origin of DACs

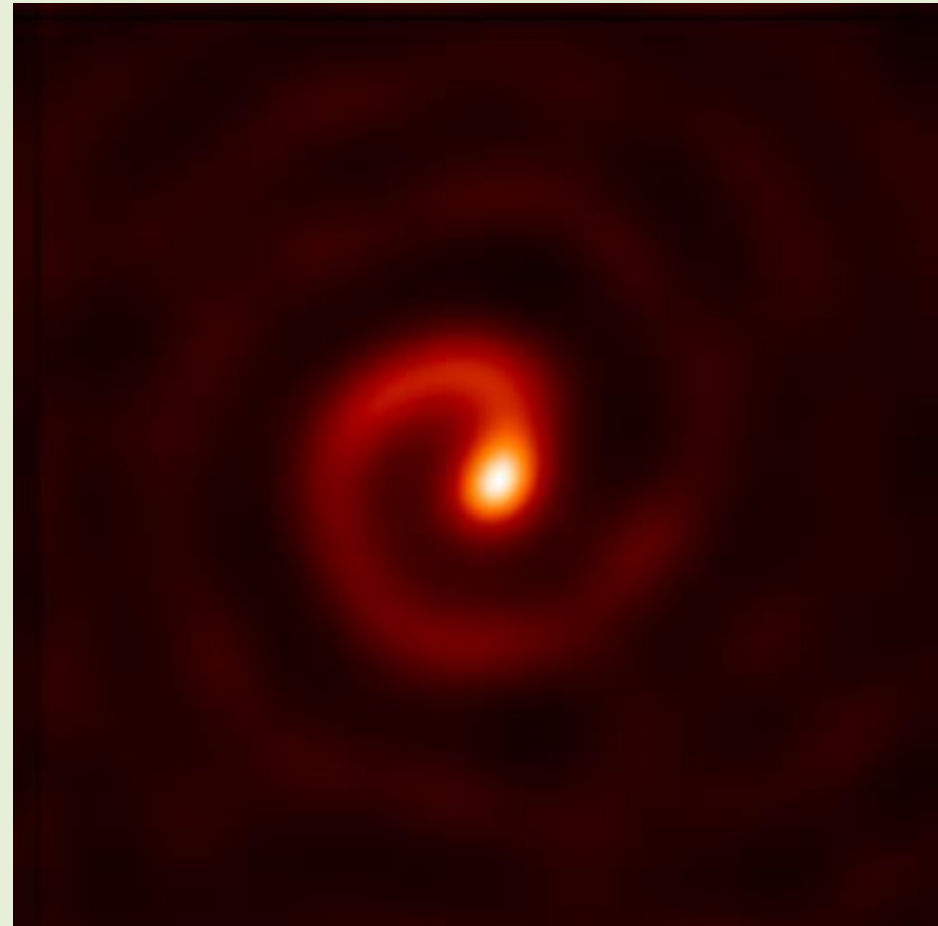
## The case of Hot Emission Stars

It has been suggested that the observed variability of mass outflows indicates **flow instabilities** (Lucy 1984; Owocki & Rybicki 1984, 1985, 1986; Lucy & Solomon 1970; MacGregor et al. 1979; Carlberg 1980; Lucy 1984; Lucy & White 1980).

### Independent and individual clouds

In the inner regions of the stellar atmosphere (from the photosphere to the first regions of the disk) of the stars that present DACs, **the plasma is ejected violently** and it does not have the form of smooth stellar wind, for as long as the phenomenon lasts.

During the e phenomenon, in the regions where the DACs are created, **the majority of plasma is distributed in the density regions** of spherical symmetry (**clouds**).



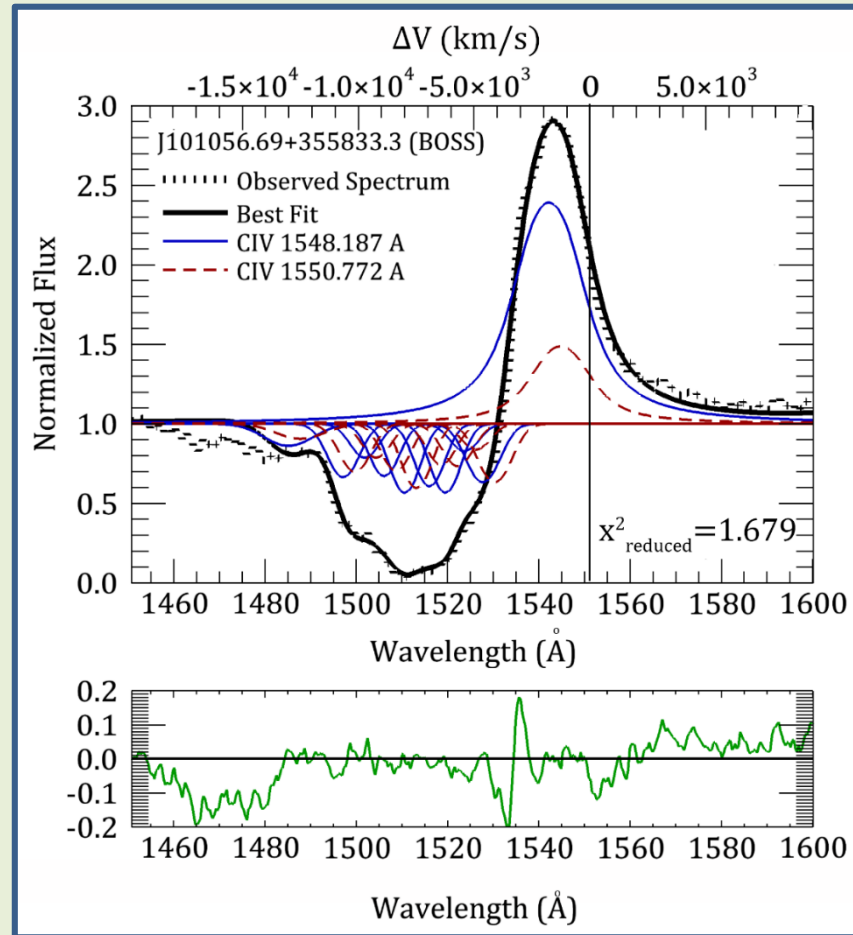
# The origin of BALs

## The case of Quasars

The “cloud” scenario seems a more plausible explanation for the formation of BAL troughs than the smooth continuous flow interpretation, due to the following reasons:

1. **BALs present complex profiles and cannot be simulated by a single known distribution (e.g. Gauss, Lorentz, Voigt etc.).** Because of this characteristic, it has been proposed that **BALs consist of a series of absorption components produced by independent** absorbing regions that cover the continuum and/or emission line region along our line of sight (\*). These absorbing regions, called clouds, are moving radially, exhibiting negligible rotation and can be thought as overdensities or density enhancements in a wind [or interacting with the wind (Weyman, et al. 1985; Filiz Ak, et al. 2012)] produced by an accretion disc.

(\*) McKee, & Tarter 1975; Turnshek 1984; Lyratzi et al. 2009, 2010, 2011; FilizAk et al. 2012; Hamann et al. 2013; Capellupo, Hamann & Barlow 2014; Misawa et al. 2014; Stathopoulos et. al. 2016, Stathopoulos et. al. 2017 , Stathopoulos et al. MNRAS, 2019

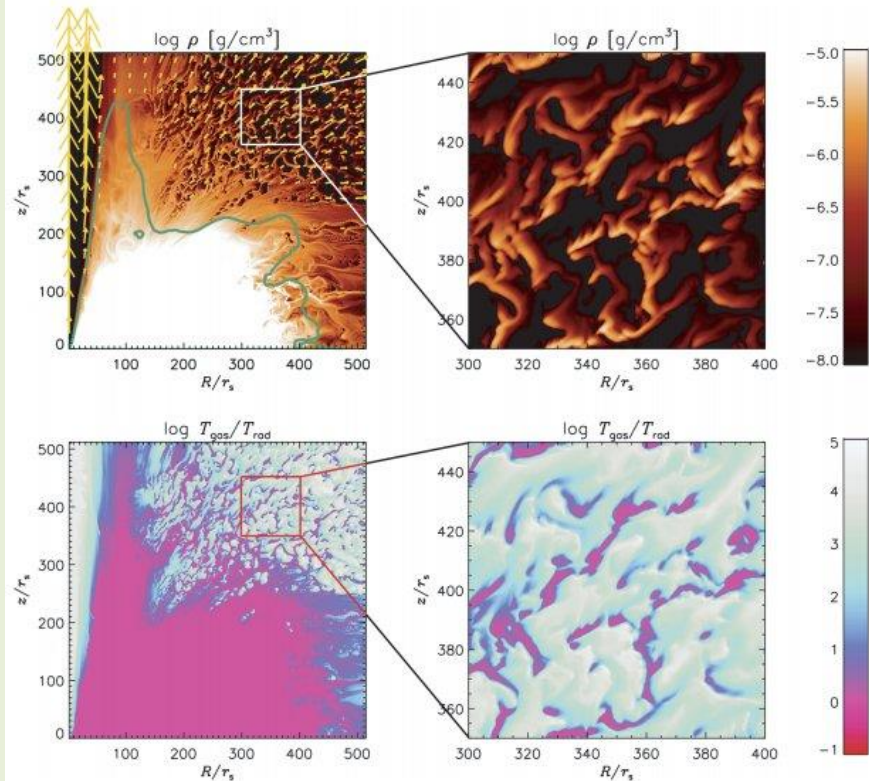




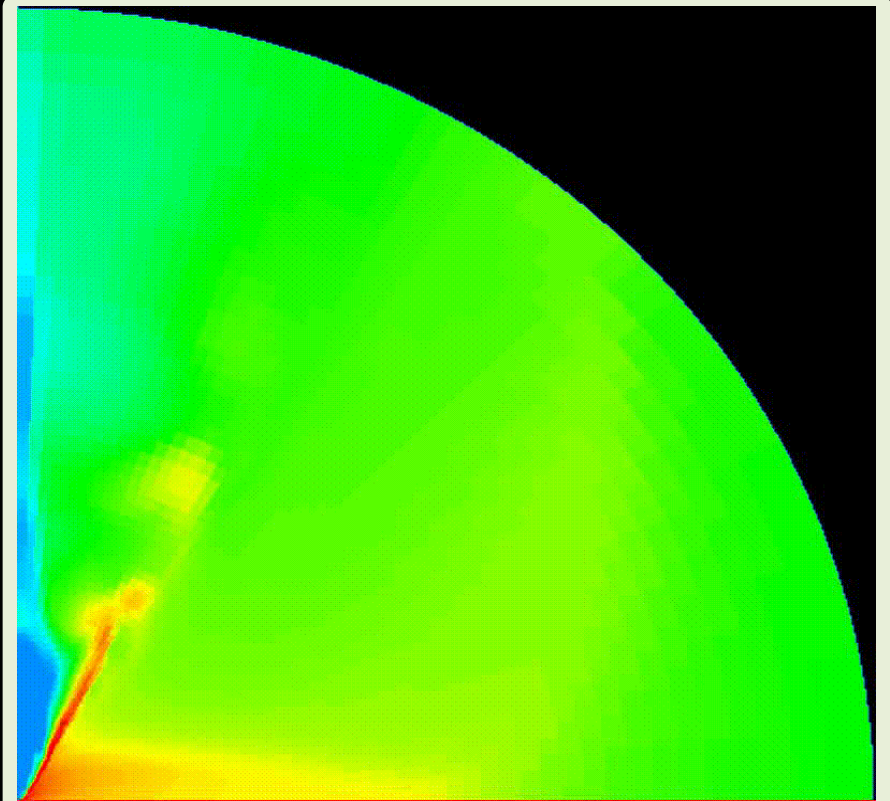
# The origin of BALs

## The case of Quasars

2. From a theoretical point of view, **clumpy outflows due to instabilities in the highly turbulent medium have been** predicted by both Takeuchi, Ohsuga & Mineshige (2013) and Waters & Proga (2016).



Takeuchi, Ohsuga & Mineshige (2013)



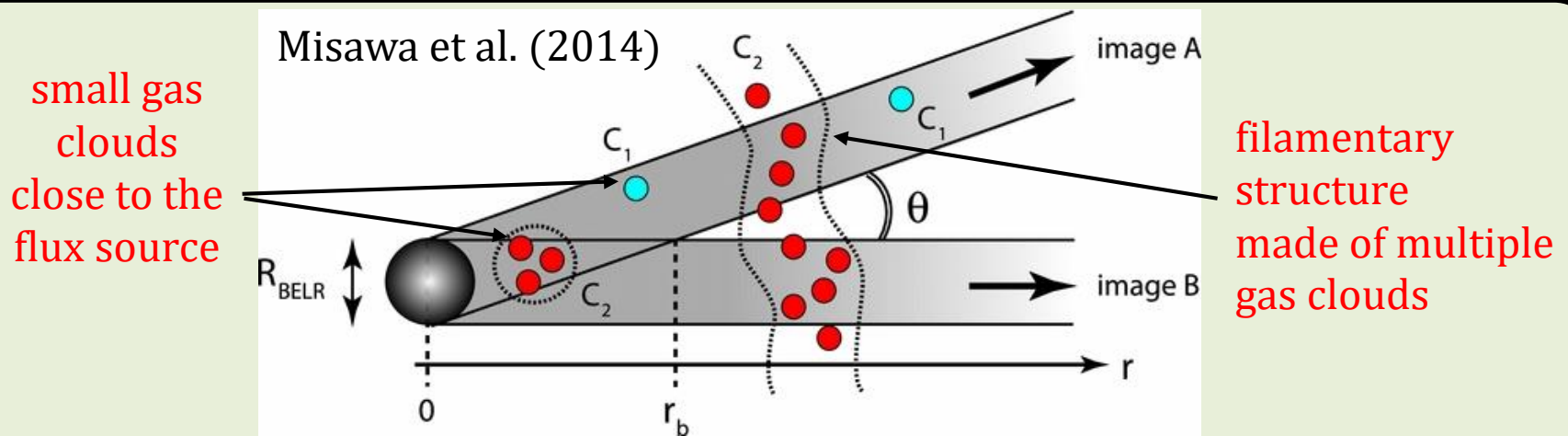
Proga et al. (2008)



# The origin of BALs

## The case of Quasars

3. Misawa et al. (2014) by observing multiple sightlines with the aid of strong gravitational lensing resolved the clumpy structure of the outflow winds in the quasar SDSS J1029+2623. Through their observations they **rejected the hypothesis of a smooth homogenous outflow and concluded to complex small structures inside the outflow** from the galactic nucleus. They proposed two different structures for the clumpy outflow: a) **small gas clouds close to the flux source** and b) **filamentary (or sheet-like) structure made of multiple clumpy gas clouds**.



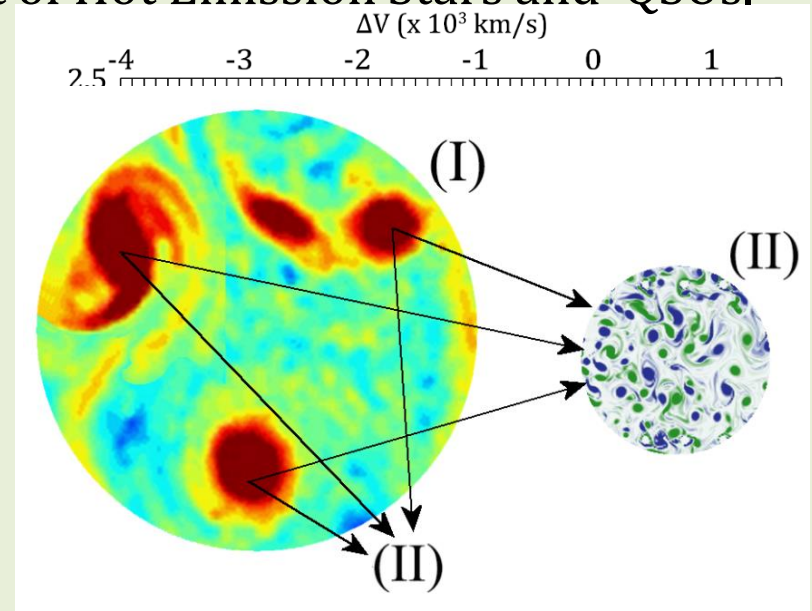
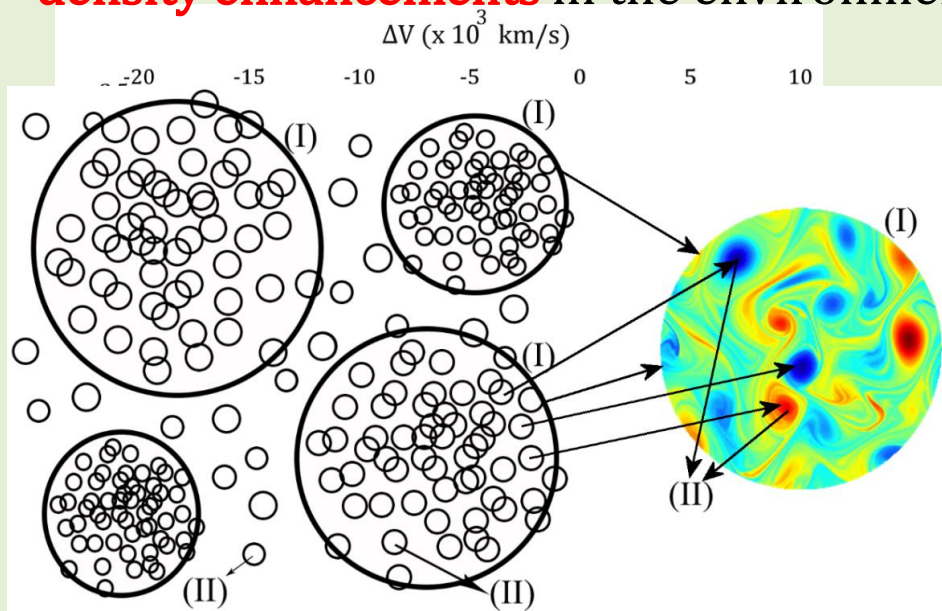
Possible locations of the  $C_1$  and  $C_2$  absorbers toward our sightlines. The large sphere represents the broad emission line region as a background flux source, while small blue and red filled circles are the  $C_1$  and  $C_2$  absorbers. The  $C_1$  absorber is always located on only the sightline toward image A, regardless of its distance.  $C_2$  is located on both sightlines toward images A and B or has a filamentary (or sheet-like) structure consisting of a number of small clumpy clouds. The boundary distance ( $r_b$ ) is the distance at which the two sightlines become fully separated with no overlap (Misawa et al. 2014).

# Hot Emission Stars and BAL Quasars

## Similar phenomena

In the spectra of **Hot Emission Stars (Be and Oe Stars)** and **BAL Quasars (BALQSOs)** we detect **similar phenomena**. This means that they may be **studied and analyzed in the same way**, taking into consideration the different scale.

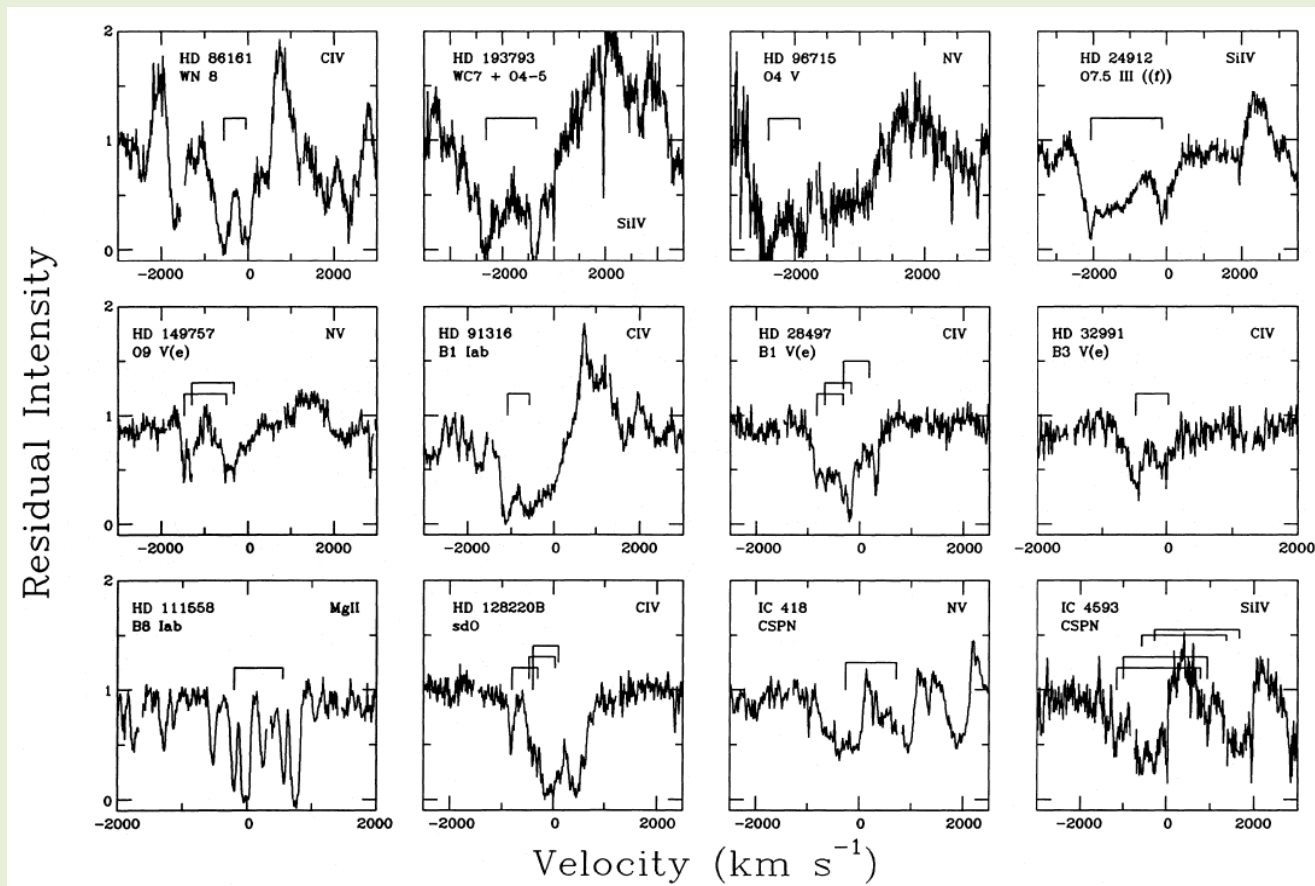
1. In both Hot Emission Stars and BAL QSOs spectra we observe **broad and complex absorption troughs** (DACs/BALs) blueshifted with respect to the emission.
2. In both cases these **broad absorption troughs can be analyzed in a series of absorption components**.
3. It has been proposed that the observed **broad absorption troughs arise from density enhancements** in the environment of Hot Emission Stars and QSOs.



# BAL Quasars and Hot Emission Stars

## Similar phenomena

Besides Hot Emission Stars and BAL Quasars, we observe similar broad absorption lines (DACs/BALs) in the spectra of other types of stars, e.g. **Wolf Rayet** and **Cataclysmic Variables** (Stathopoulos et. al. 2016, 2017, 2019 (MNRAS)).



IUE spectra illustrating DACs in WR, O, B, Be, SdO and CSPN stars (Prinja 1990).

# Study of DACs and BALs

According to the cloud scenario, **DACs/BALs result from the synthesis of many individual components**, which are created in different absorbing regions (clouds) which are in the line of sight.

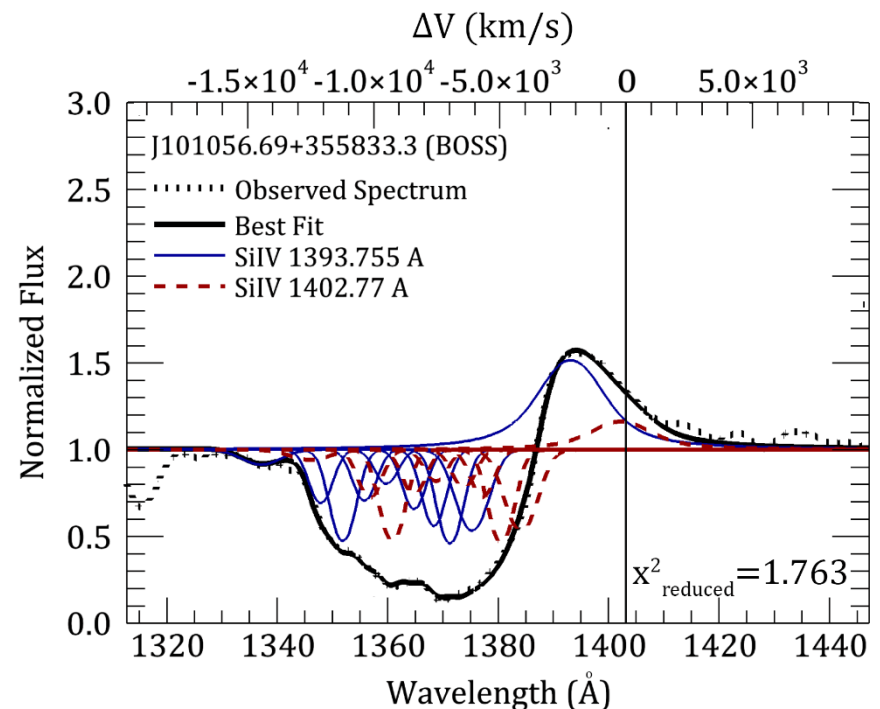
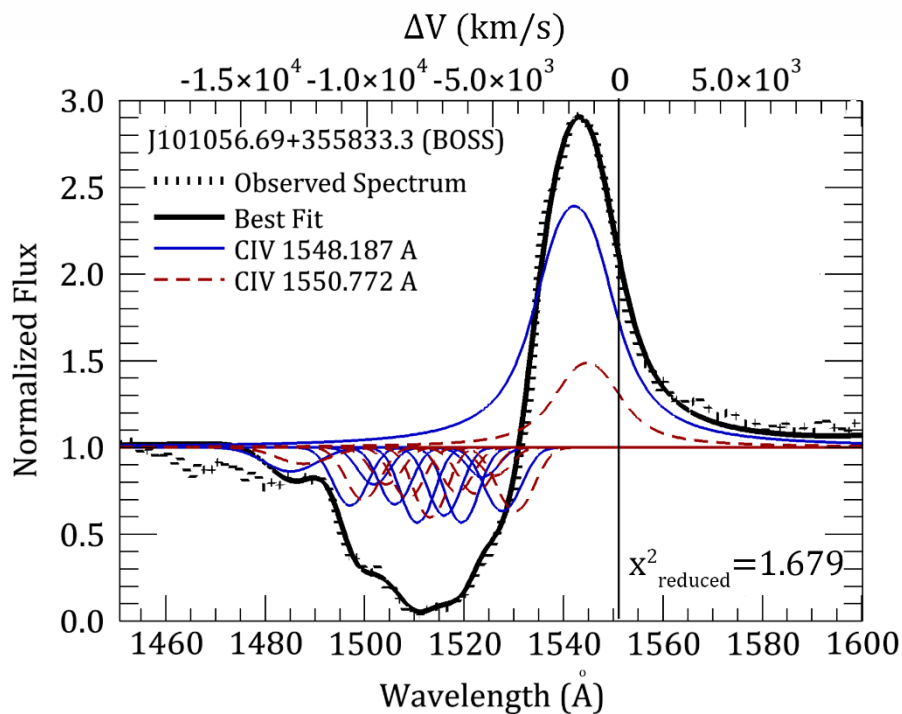
In order to study the complex profiles of DACs/BALs and the kinetics of the clouds, **we apply the GR** model (Danezis et al. 2003, 2007, 2009; Lyratzi et al. 2007, 2009; Sthapopoulos et al. 2015, 2019) with which we are able to:

1. **analyze the DACs/BALs** profiles to their components.
2. **calculate a series of physical** parameters (such as the radial velocity, the FWHM, the optical depth at line center and the column density), which are characteristic of the density regions where DACs/BALs are created.

For this analysis **we use the ASTA software** which is the only software that incorporates the GR model (Tzimeas et al 2018).

# Main advantages of the GR model

1. With GR model the observed DAC/BAL trough is not studied as a unique line. On the contrary, the great advantage of the model is that the observed DAC/BAL profile can be analyzed to its components so each DAC/BAL component can be studied separately. This means that the DAC/BAL trough is not studied as a whole, but in parts. However, these parts are not arbitrarily selected, but each one of them is an actual absorption component which is created by a real physical structure. So, each actual absorption component of a DAC/BAL can be studied independently.





# Main advantages of the GR model

2. The **variability of the absorption components** of the DAC/BAL troughs, which is measured in this way, **corresponds to the variation of the properties of the physical structure** that creates the observed absorption and lead us to conclusions about the existence (or not) of the clouds.
3. GR model ensures the **uniqueness of the number of DAC/BAL components** as well as the **uniqueness of the calculated values of the physical** parameters (radial velocity, FWHM, optical depth, column density etc.), through **specific and strong criteria that apply in the case of resonance lines** (Stathopoulos et al. 2015, 2019).



# Our team's project

This study is a small part of a project of our scientific team, which aims to **analyze the observed absorption and emission profiles** (DACs, DEC, BALs, BELs) of **many ions** in **many kinds of objects**, such as Hot Emission Stars, Wolf Rayet Stars, Cataclysmic Variables and BAL Quasars, applying the GR model and using the ASTA software.

Through our study on the time variability of the calculated physical parameters, **we intend to confirm the existence of the clouds** in all types of the studied objects and to draw **statistical conclusions**.

In this part of our work we **analyze the Si IV and C IV profiles** in two different spectra of a Be Star, a Wolf Rayet Star, a Cataclysmic Variable and a BAL Quasar. We **study the variability of these profiles through the variability of the calculated parameters**, such as the radial velocity, the FWHM, the optical depth and the column density.

**DACs: Discrete Absorption Components**

**DEC : Discrete Emission Components**

**BALs: Broad Absorption Components**

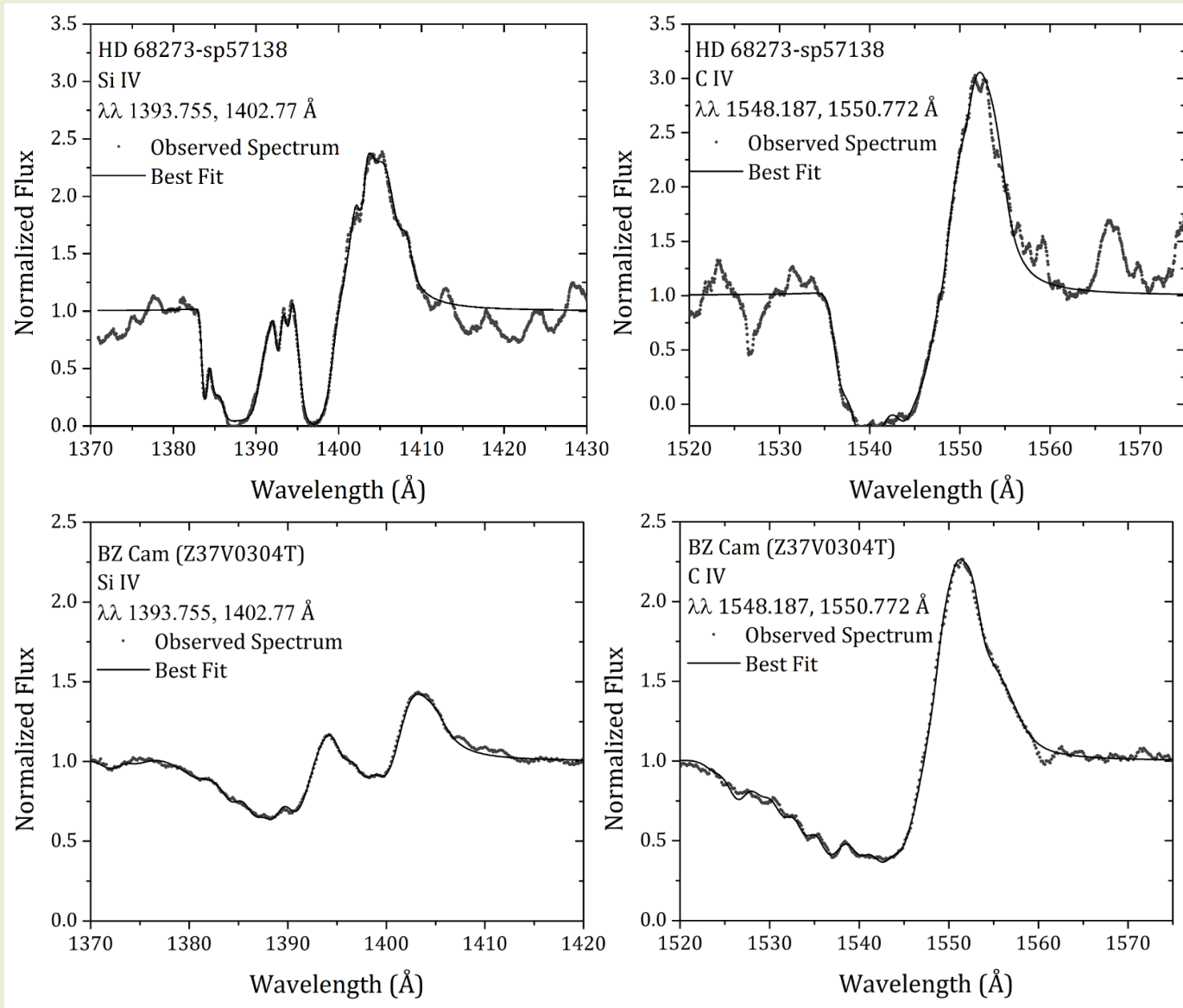
**BELs: Broad Emission Components**

# Data

Object	Type	Spectrum	Date
HD 37128 - $\epsilon$ Orionis	<b>B0 Ia , Hot Emission Star</b>	SWP 03536	5 Dec 1978
		SWP 24879	10 Jan 1985
J155335.78 + 324308.1	<b>Quasar</b>	1403-53227-0075	10 Aug 2004
		4966-55712-0266	31 May 2011
HD 68273 - $\gamma$ Velorum	<b>Wolf Rayet Star</b>	SWP 42783	22 Oct 1991
		SWP 57138	15 May 1996
BZ_Cam	<b>Cataclysmic Variable Star</b>	Z37V0304T	31 Aug 1996, 21:37:04
		Z37V0306T	31 Aug 1996, 22:56:16

# Best fits of Si IV and C IV

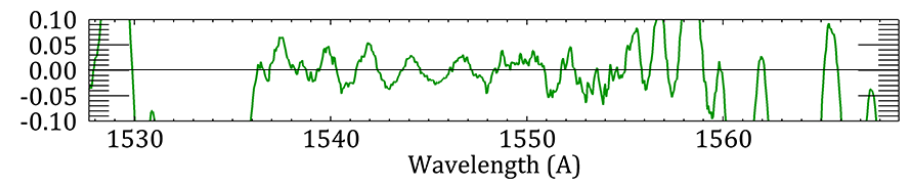
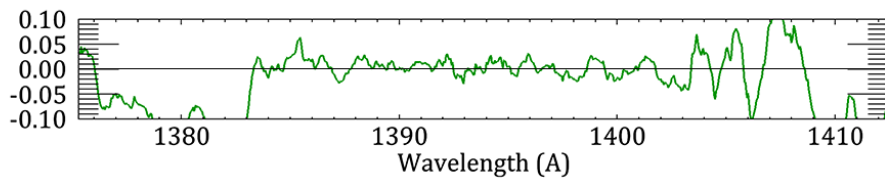
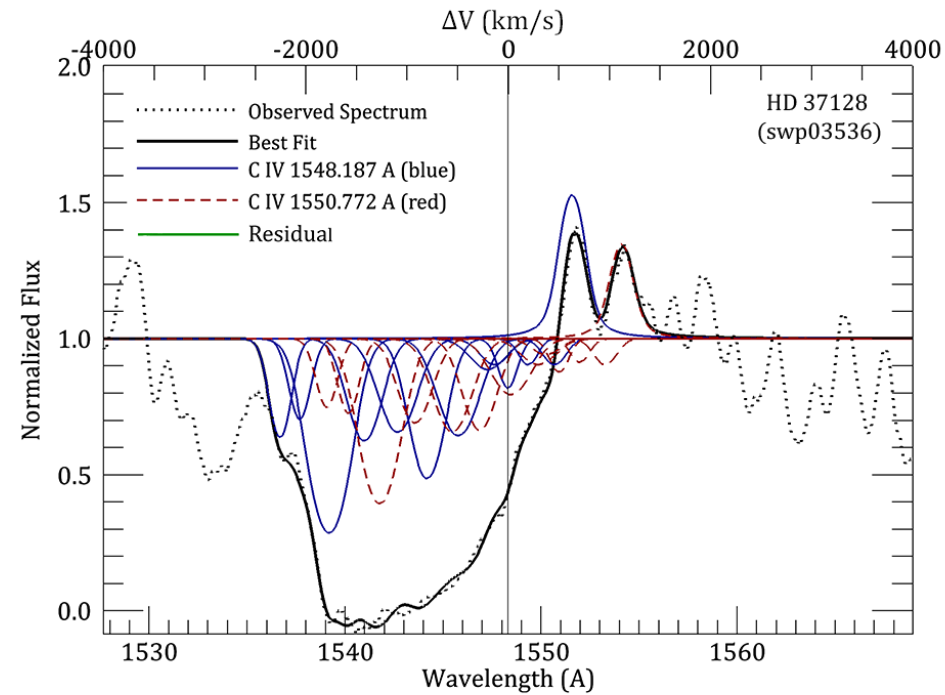
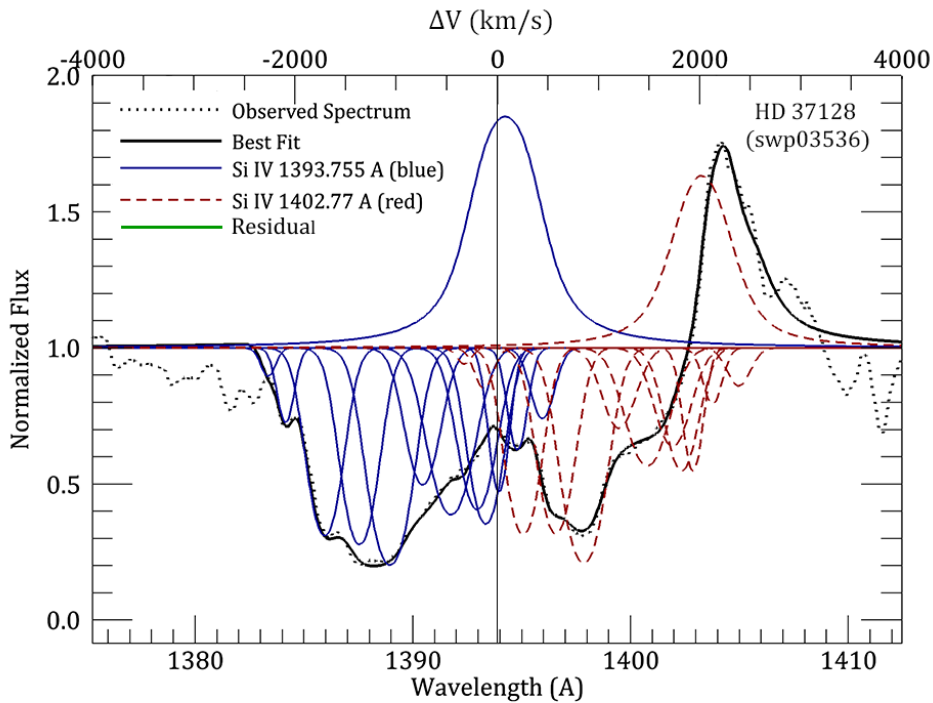
in the cases of the Wolf Rayet (up) and the Cataclysmic Variable (down)



Dotted Line: Observed Spectrum

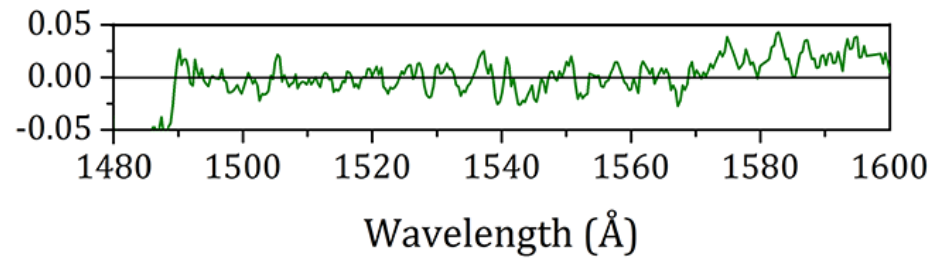
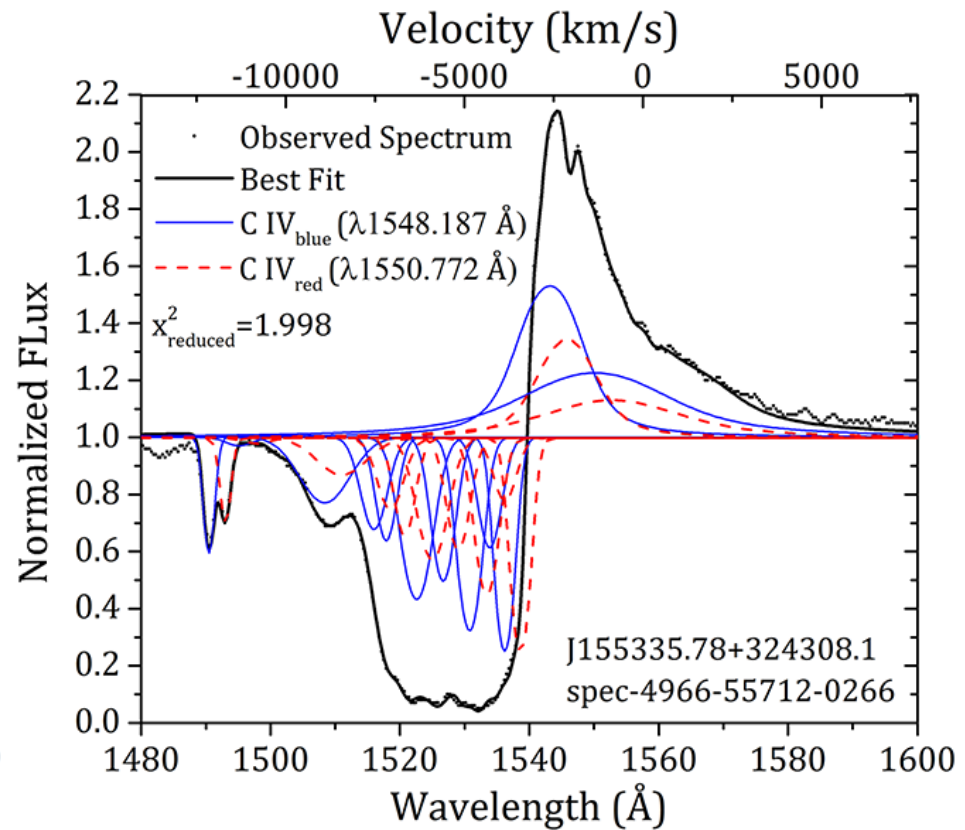
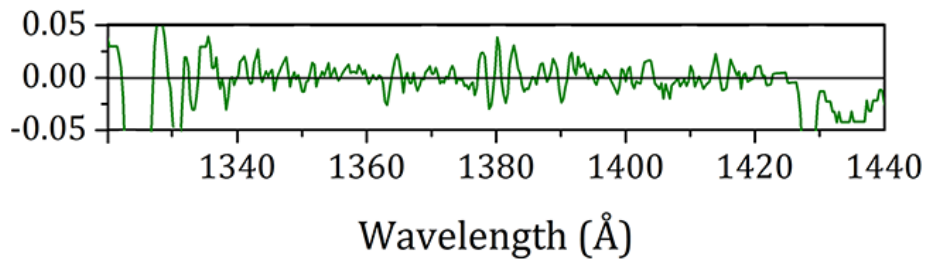
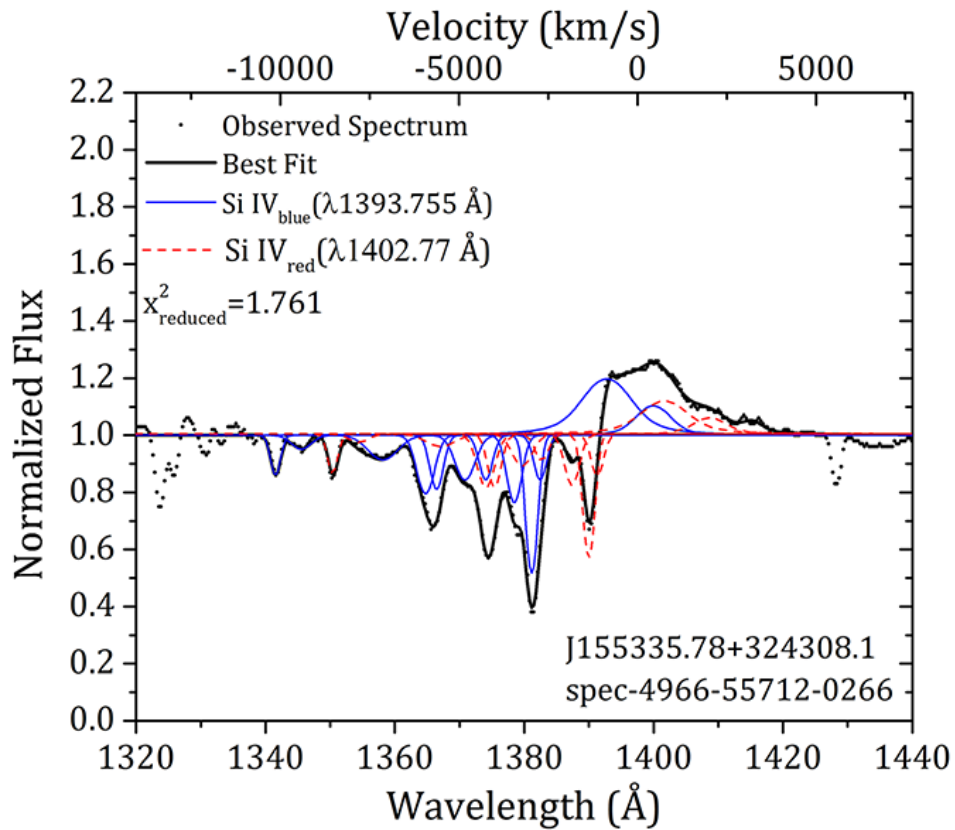
Thick Black Line: Best Fit

# Best fits and analysis of Si IV and C IV in the case of the Hot Emission Star



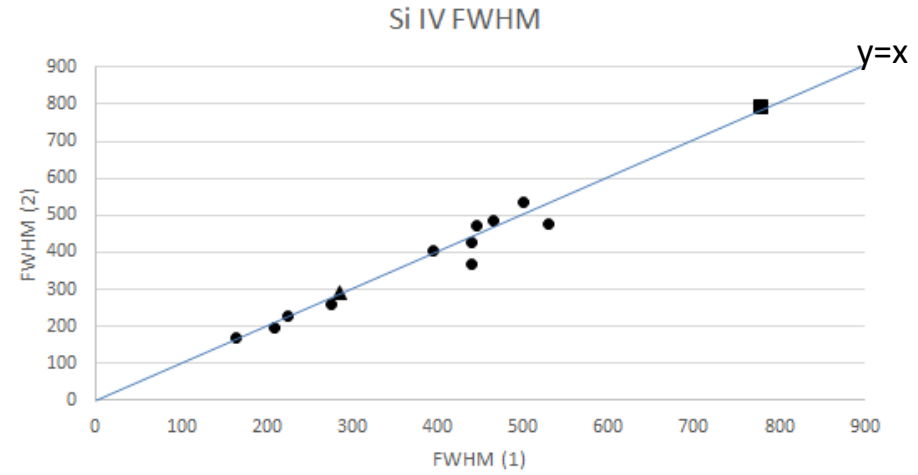
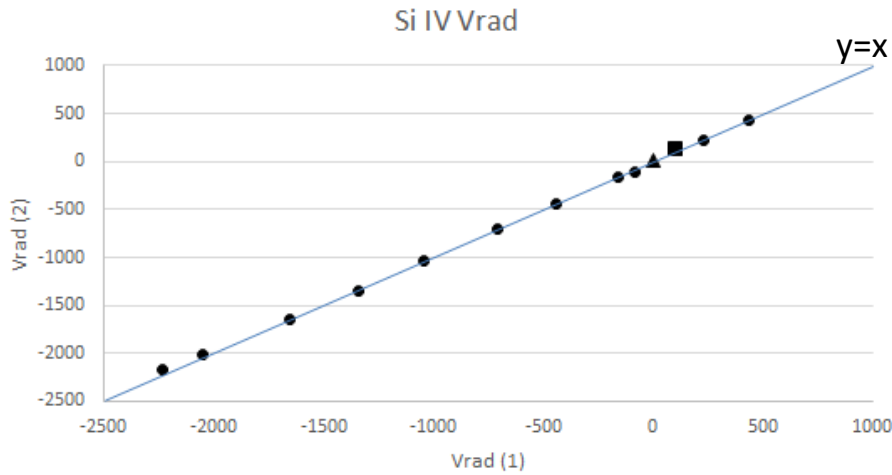
- Dotted Line: Observed Spectrum
- Thick Black Line: Best Fit
- Blue Line: Shorter wavelength member of the doublet
- Red Line: Longer wavelength member of the doublet
- Green Line: Residual

# Best fits and analysis of Si IV and C IV in the case of the Quasar

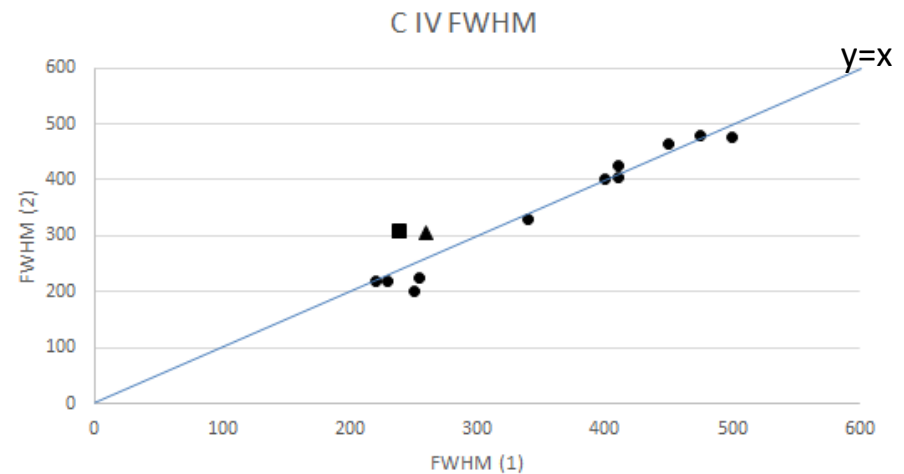
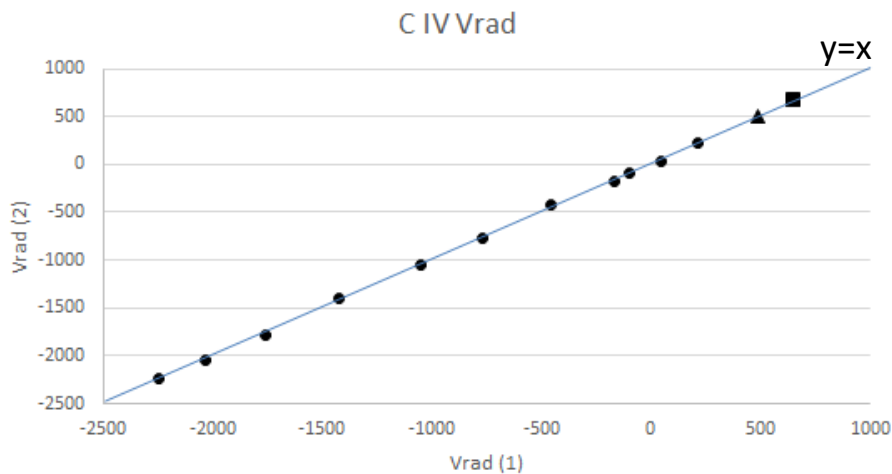


# HD 37128 - $\epsilon$ Orionis B0 Ia (Hot Emission Star)

## Si IV



## C IV



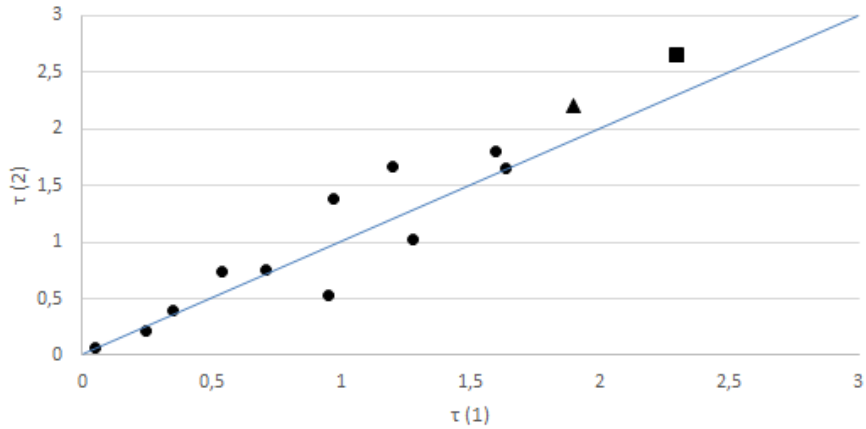
Comparison of the values of Vradial (left) and FWHM (right), derived from the two spectra. We observe no variation in the radial velocity and small variations in the FWHM of a few components.



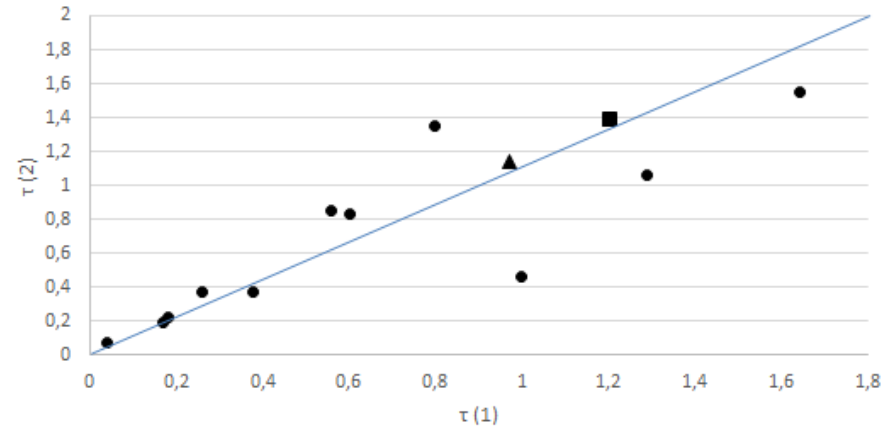
# HD 37128 - $\epsilon$ Orionis B0 Ia (Hot Emission Star)

## Si IV

Si IV Optical Depth (blue)

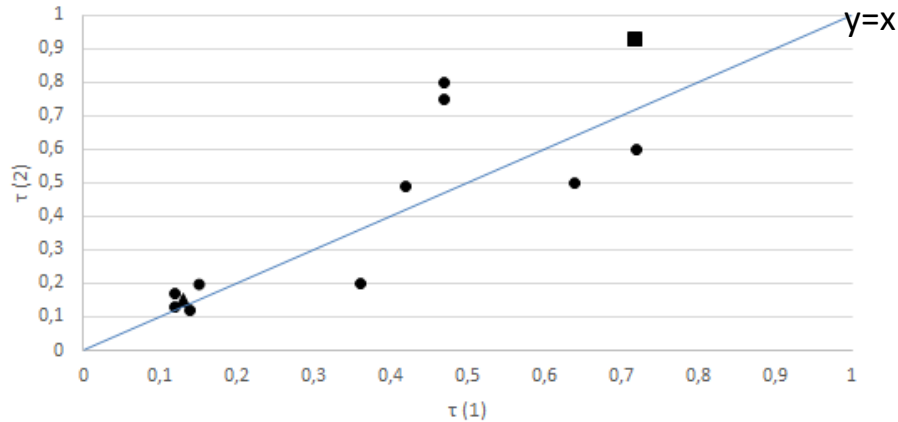


Si IV Optical Depth (red)

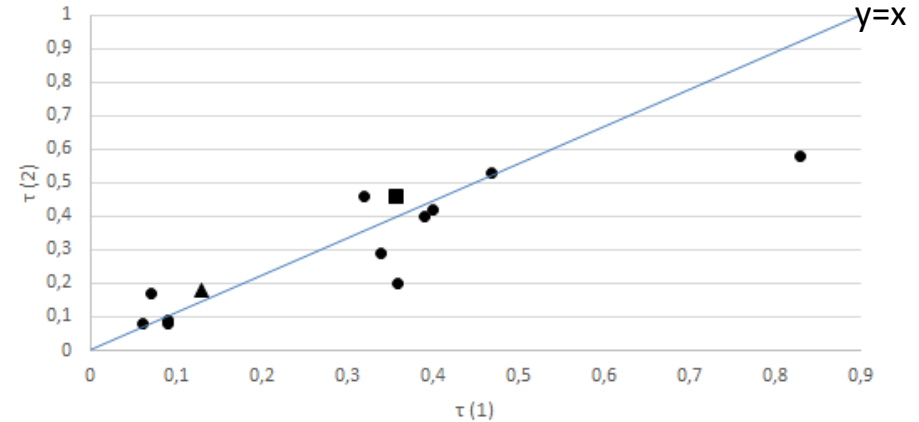


## C IV

C IV Optical Depth (blue)



C IV Optical Depth (red)

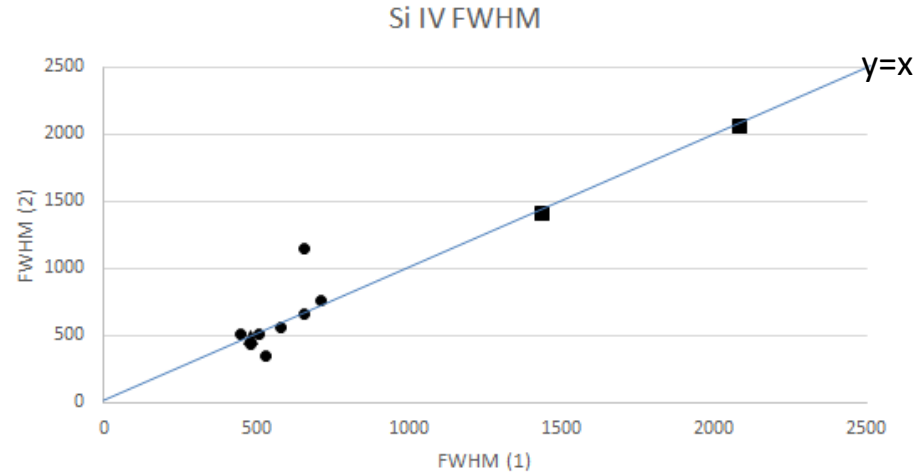
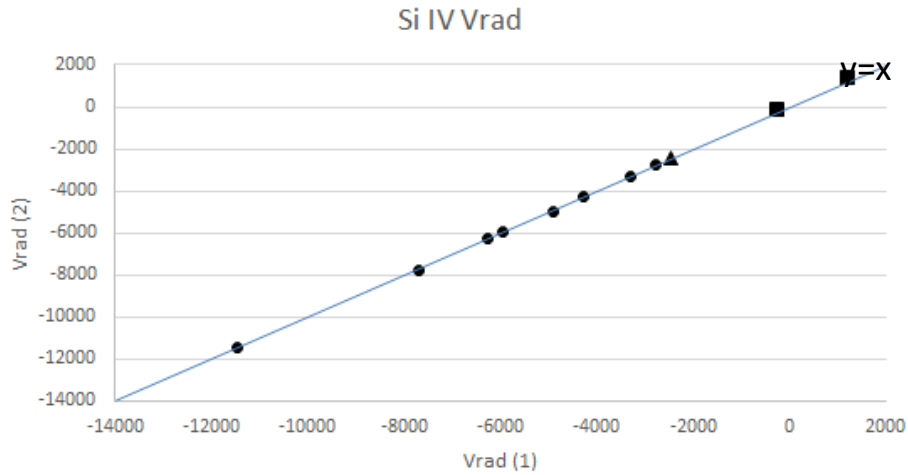


Comparison of the values of the optical depth at line center of the blue (left) and the red (right) components, derived from the two spectra. We observe variation in most components.

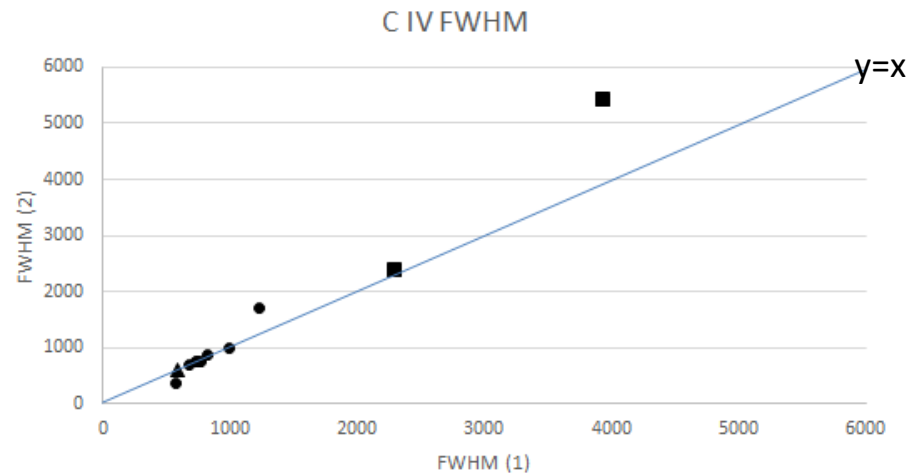
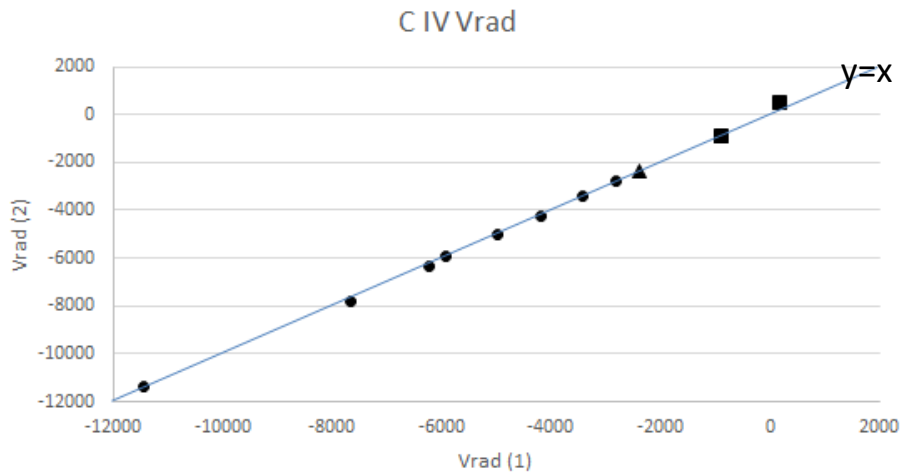


# J155335.78 + 324308.1 (Quasar)

## Si IV



## C IV

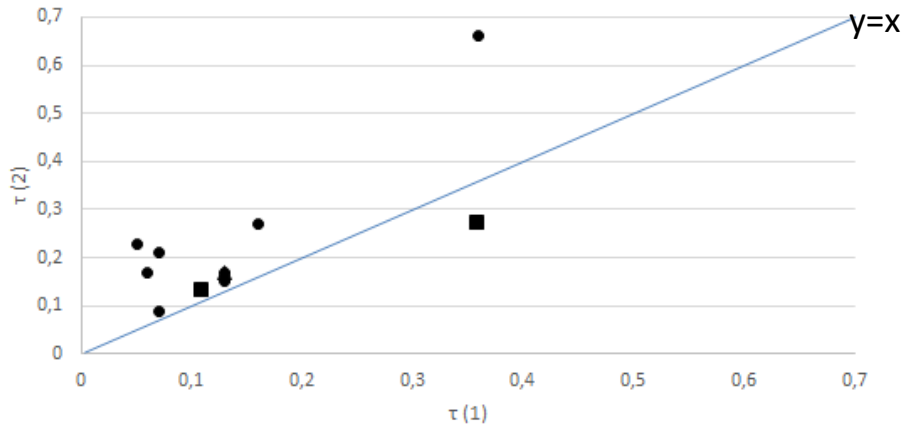


Comparison of the values of Vradial (left) and FWHM (right), derived from the two spectra. We observe no variation in the radial velocity and small variations in the FWHM of a few components.

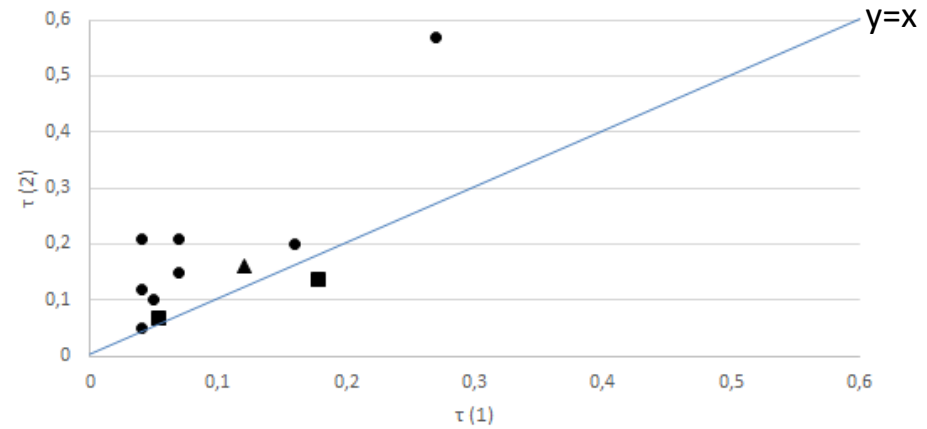
# J155335.78 + 324308.1 (Quasar)

## Si IV

Si IV Optical Depth (blue)

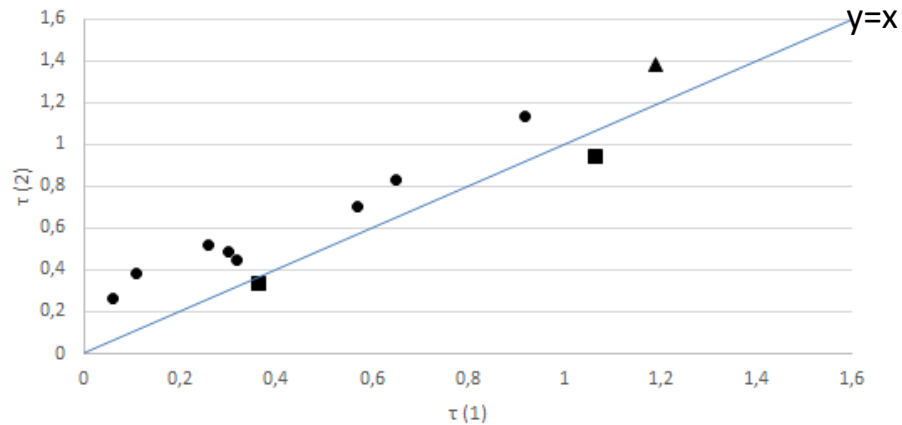


Si IV Optical Depth (red)

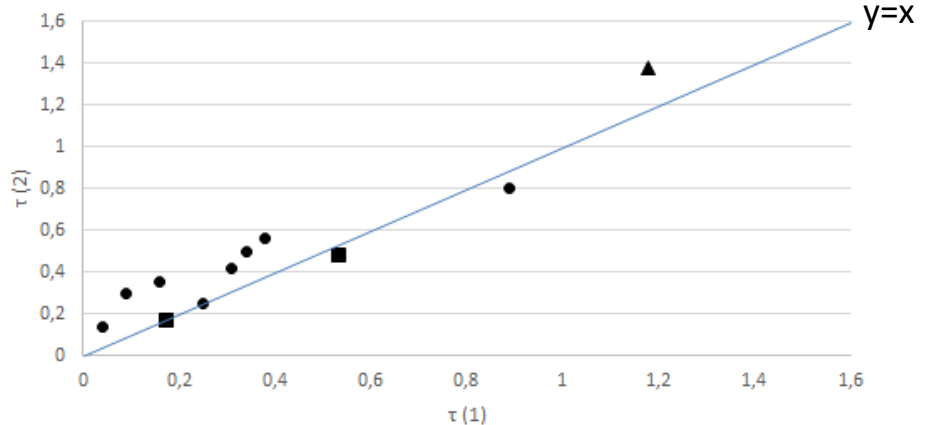


## C IV

C IV Optical Depth (blue)



C IV Optical Depth (red)

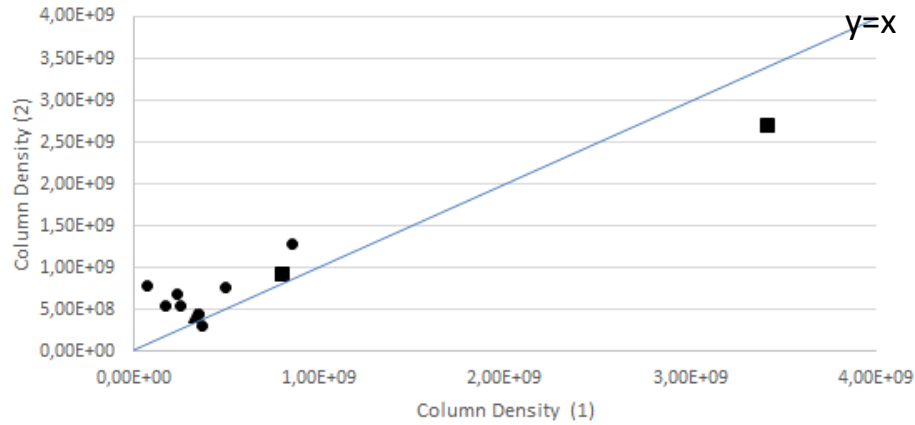


Comparison of the values of the optical depth at line center of the blue (left) and the red (right) components, derived from the two spectra. We observe variation in most components.

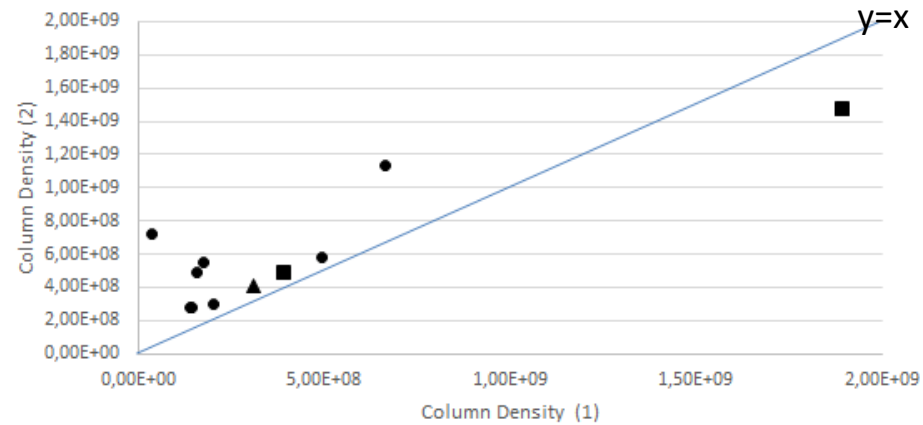
# J155335.78 + 324308.1 (Quasar)

## Si IV

Si IV Column Density (blue)

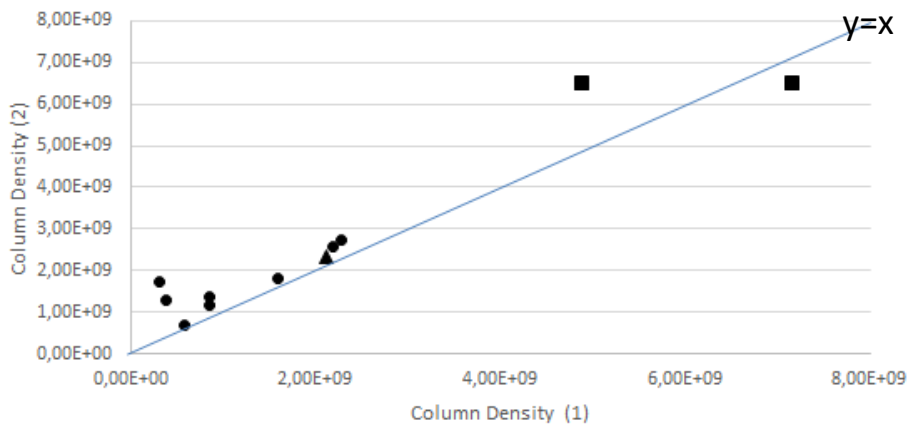


Si IV Column Density (red)

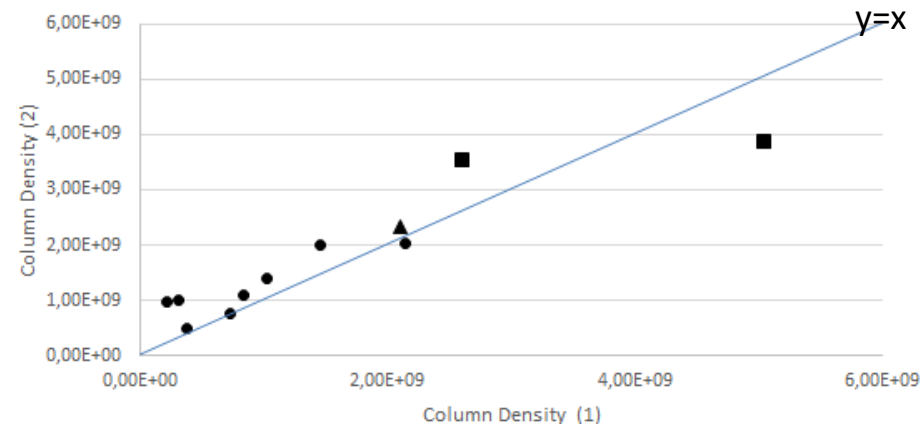


## C IV

C IV Column Density (blue)



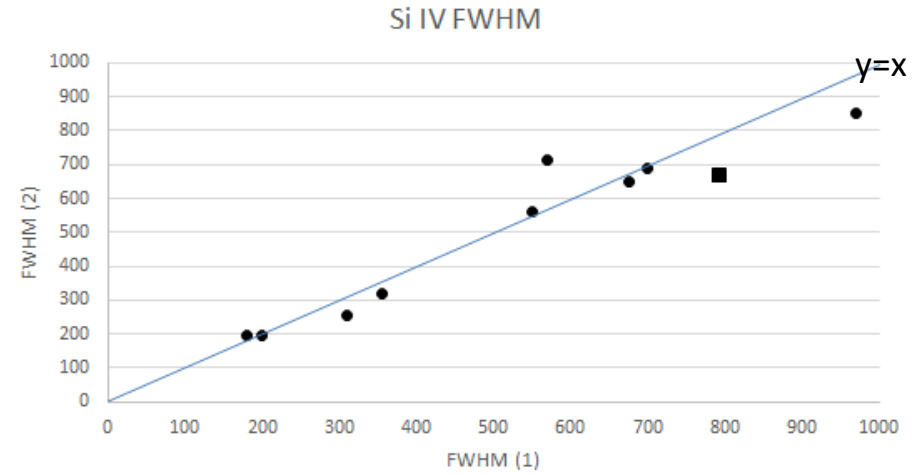
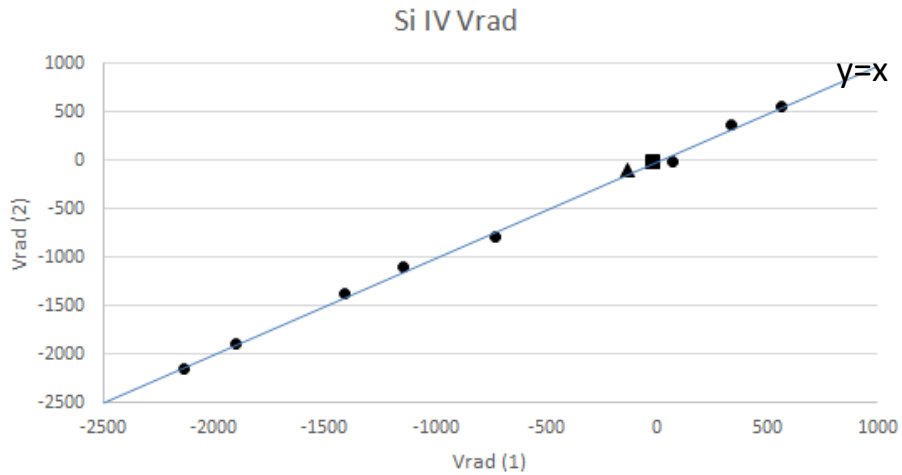
C IV Column Density (red)



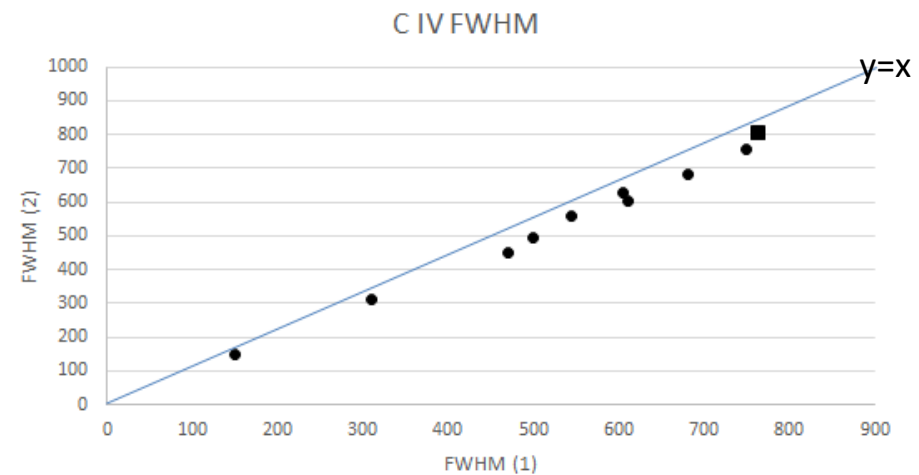
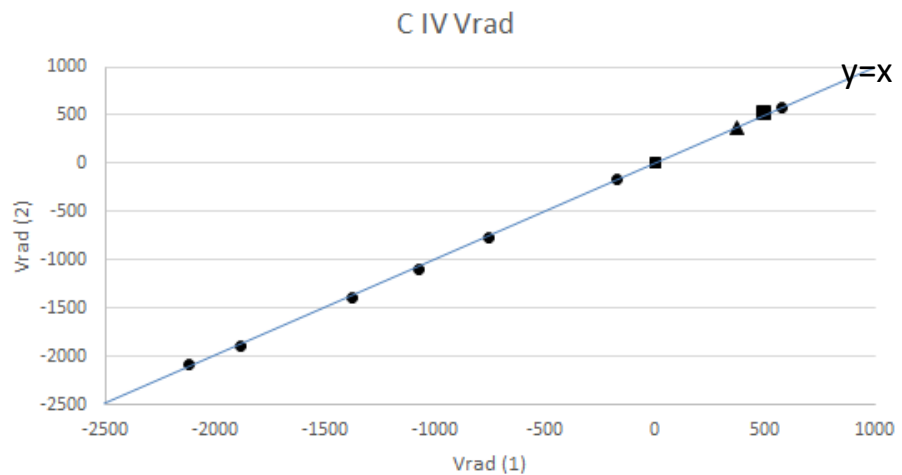
Comparison of the values of the column density of the blue (left) and the red (right) components, derived from the two spectra. We observe variation in most components.

# HD 68273 - $\gamma$ Velorum (Wolf Rayet Star)

## Si IV



## C IV



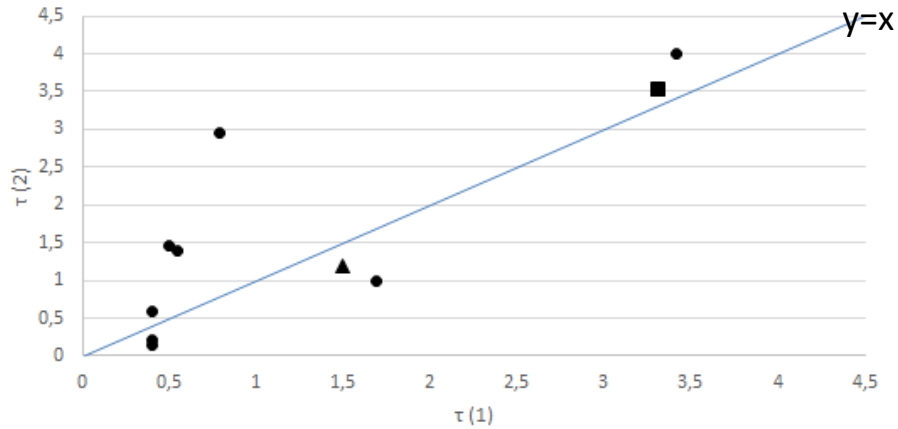
Comparison of the values of Vradial (left) and FWHM (right), derived from the two spectra. We observe no variation in the radial velocity and small variations in the FWHM.



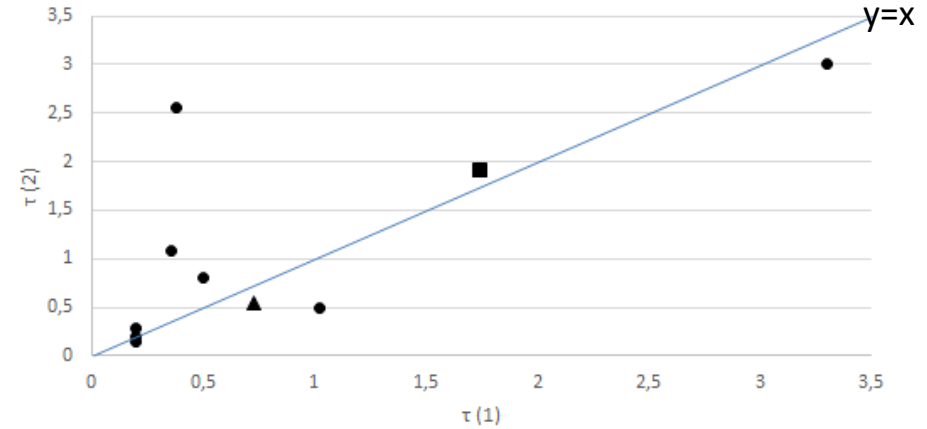
# HD 68273 - $\gamma$ Velorum (Wolf Rayet Star)

## Si IV

Si IV Optical Depth (blue)

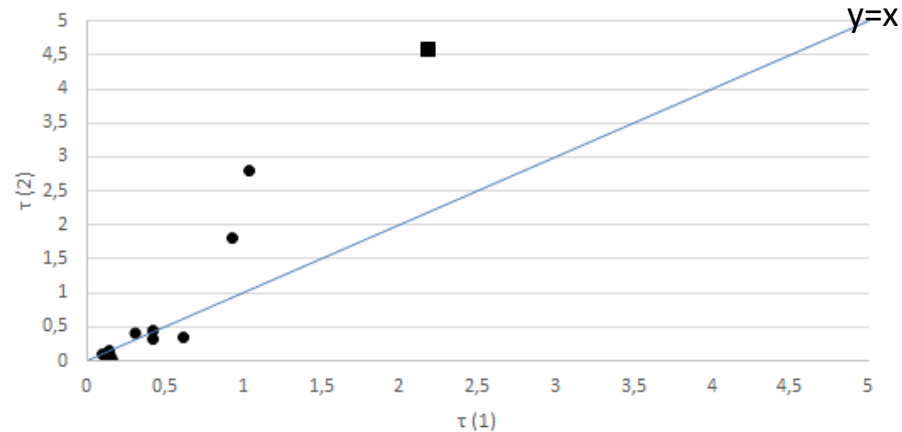


Si IV Optical Depth (red)

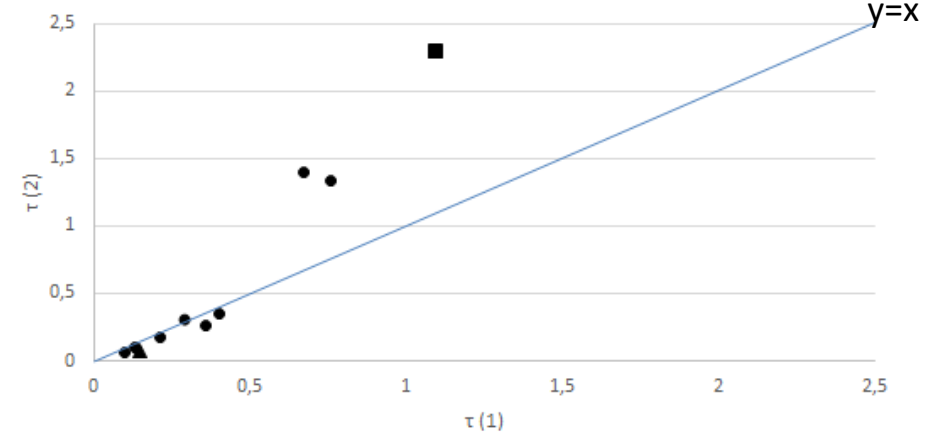


## C IV

C IV Optical Depth (blue)



C IV Optical Depth (red)

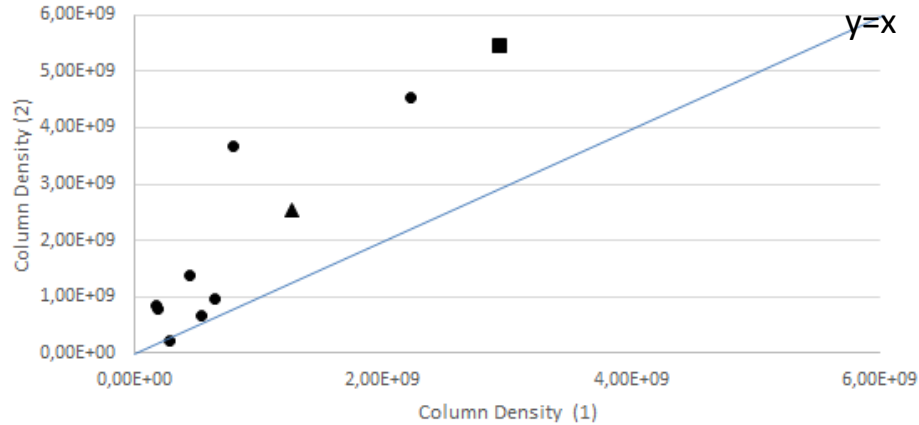


Comparison of the values of the optical depth at line center of the blue (left) and the red (right) components, derived from the two spectra. We observe variation in most components.

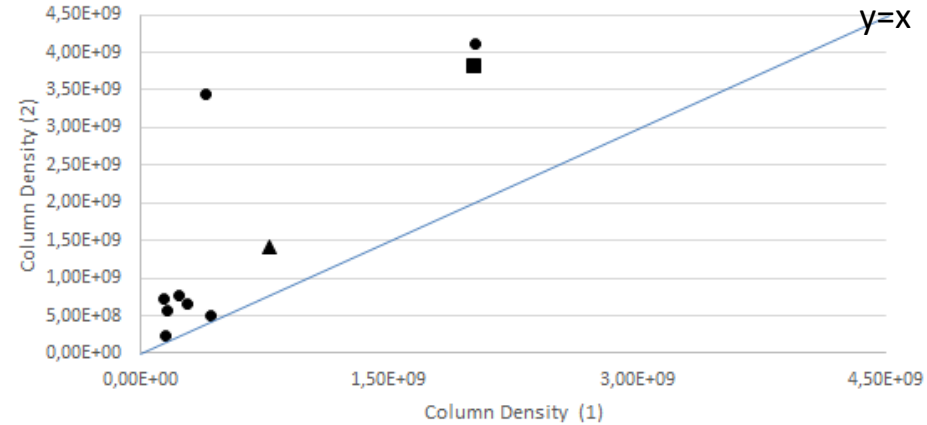
# HD 68273 - $\gamma$ Velorum (Wolf Rayet Star)

## Si IV

Si IV Column Density (blue)

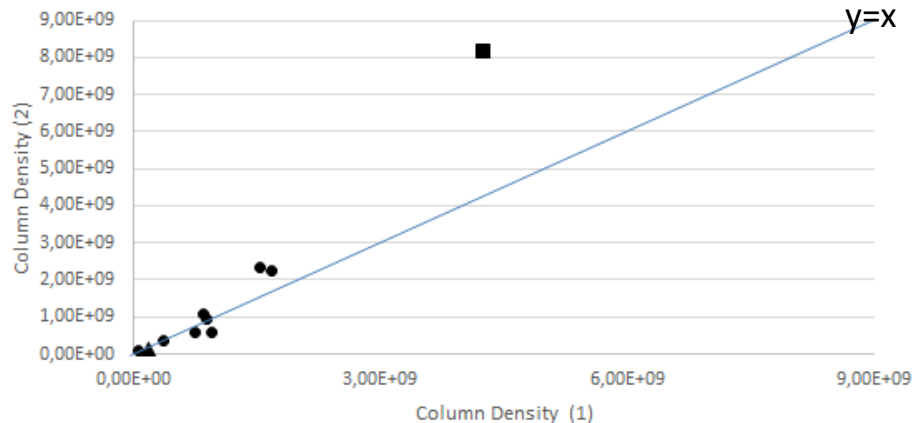


Si IV Column Density (red)

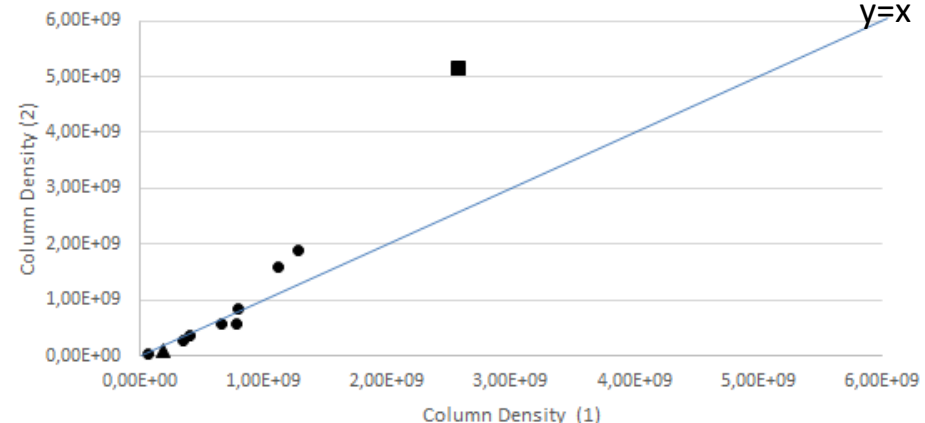


## C IV

C IV Column Density (blue)



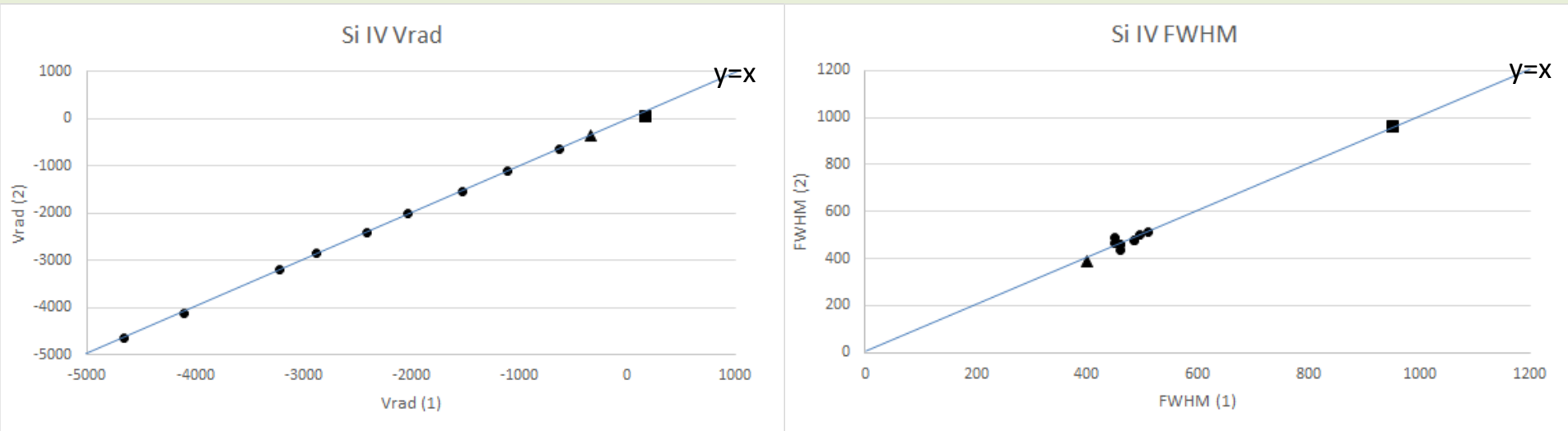
C IV Column Density (red)



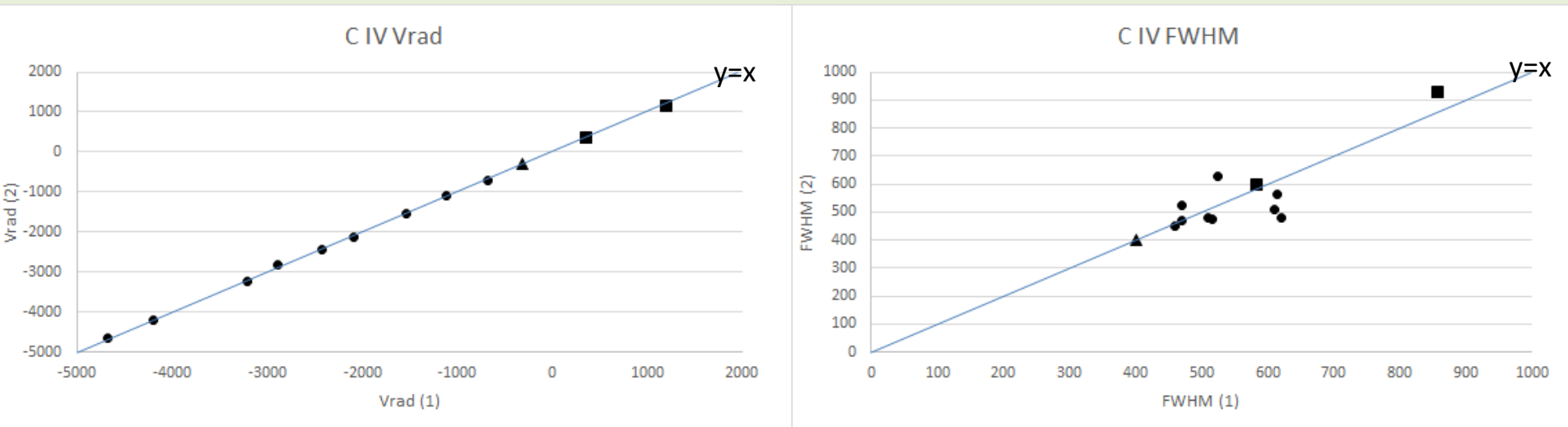
Comparison of the values of the column density of the blue (left) and the red (right) components, derived from the two spectra. We observe variation in most components.

# BZ\_Cam (Cataclysmic Variable Star)

## Si IV



## C IV

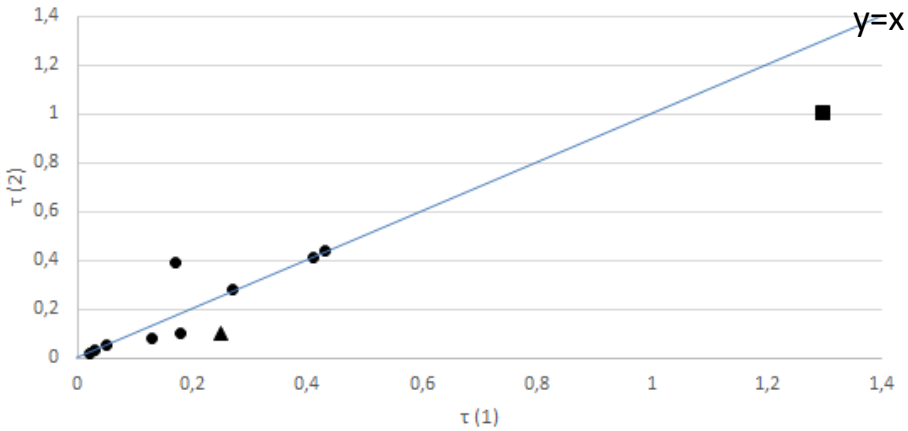


Comparison of the values of Vradial (left) and FWHM (right), derived from the two spectra. We observe no variation in the radial velocity and small variations in the FWHM of a few components.

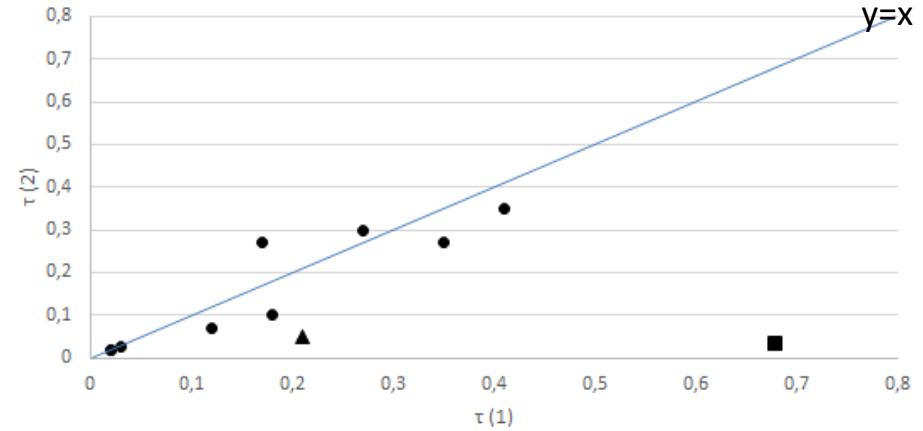
# BZ\_Cam (Cataclysmic Variable Star)

## Si IV

Si IV Optical Depth (blue)

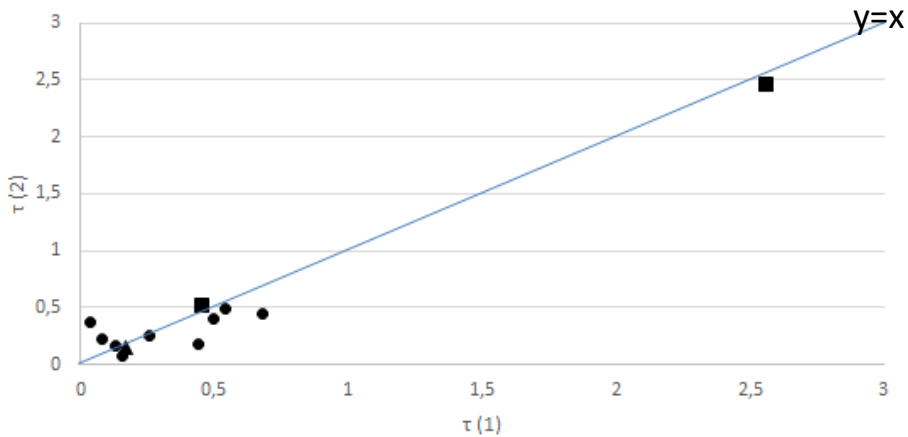


Si IV Optical Depth (red)

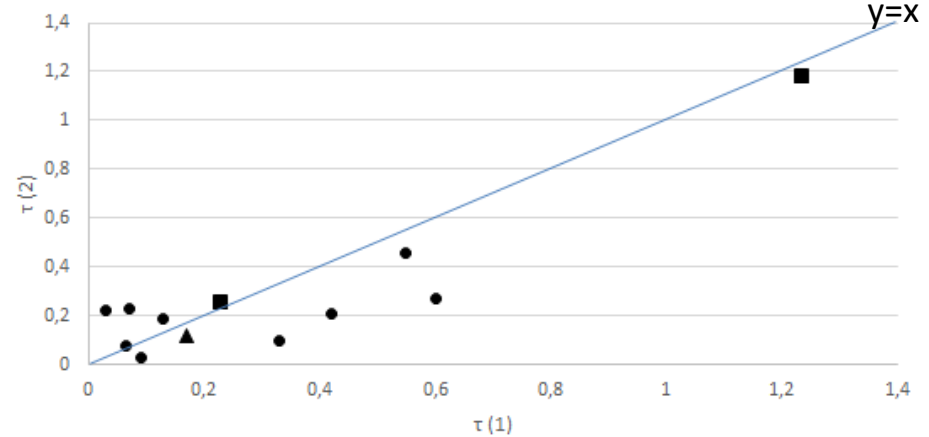


## C IV

C IV Optical Depth (blue)



C IV Optical Depth (red)

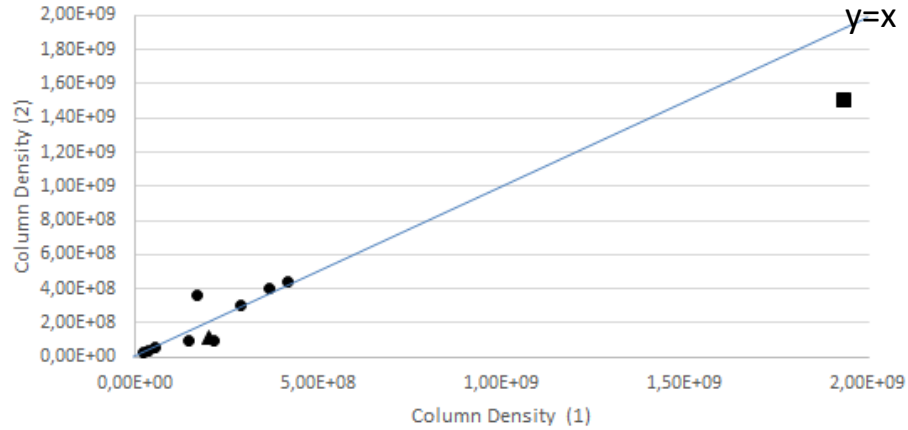


Comparison of the values of the optical depth at line center of the blue (left) and the red (right) components, derived from the two spectra. We observe variation in most components.

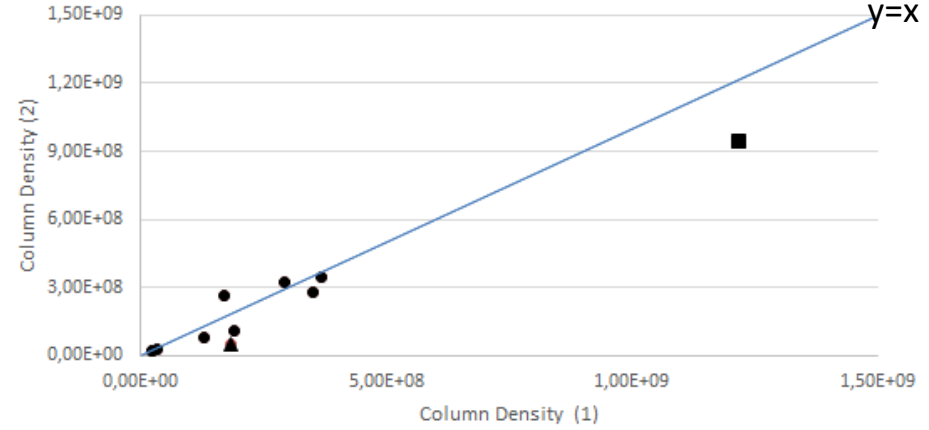
# BZ\_Cam (Cataclysmic Variable Star)

## Si IV

Si IV Column Density (blue)

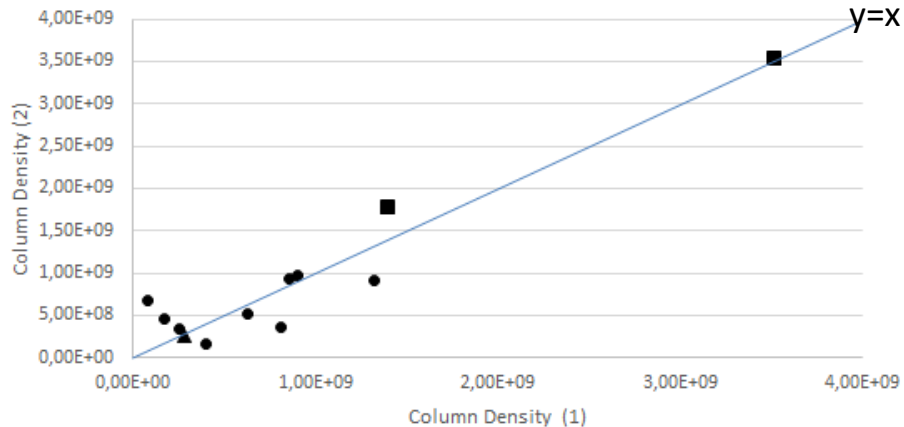


Si IV Column Density (red)

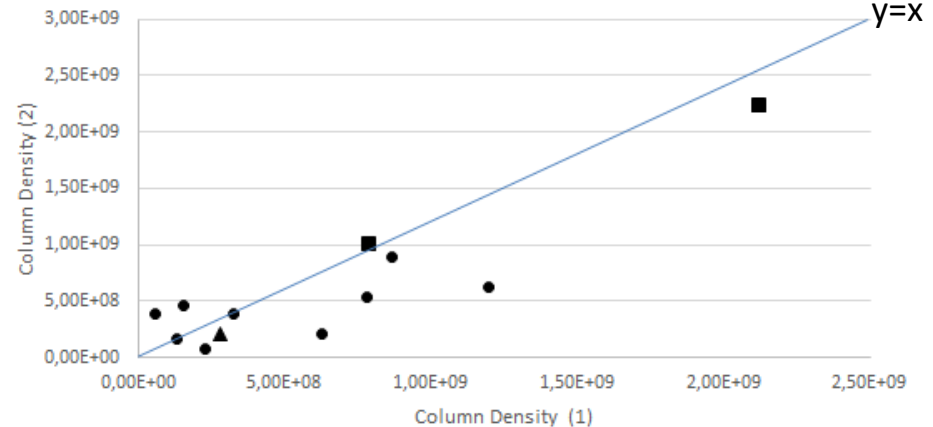


## C IV

C IV Column Density (blue)



C IV Column Density (red)



Comparison of the values of the column density of the blue (left) and the red (right) components, derived from the two spectra. We observe variation in most components.

# Conclusions

By applying the GR model using ASTA software we were able to analyze the spectra of all the four different types of the studied objects.

In all cases we were able to:

- **distinguish the individual components** that compose the final profile and
- **calculate the values of the physical parameters** of each individual component

Thus we were able to **compare individual components** between different epochs **and investigate the variability of individual structures** in the environment of the studied object. From our analysis we conclude to the following:

In all the components, in the four studied objects and for both Si IV and C IV :

1. **We did not observe any change in velocity shifts** so there is **no evidence for acceleration** of the material that creates the observed spectral lines.
2. We observed **small changes in the widths (FWHM)** of a few individual components between the two epochs.



# Conclusions

3. The vast majority of components show **variations in the optical depths at line center** and in **the column densities**. This might be due to small energy variations (changes in the ionization state of the flow), resulting to the variation of the number of the absorbers/emitters.
  - i. **None** of the studied DACs/BALs **shows variations in its entire profile**. DACs/BALs show **variations only in individual components**.
  - ii. Within the same DAC/BAL, **variable components exhibit independent variations**.
  - iii. In all the studied objects, absorption components exhibit **non coordinated variations**, i.e. components at specific velocity shifts strengthen, while components at different velocities within the same DAC/BAL weaken over time.
  - iv. Within the same object, **Si IV and C IV components** over corresponding velocities **show non coordinated variations**.

All of the above indicate the distinction and independence of absorption components, i.e. the **distinction and independence of the corresponding clouds**.

**Thank you!**